

## SUPPLEMENTARY NOTE

Alig *et al.* Distinct Hodgkin lymphoma subtypes defined by noninvasive genomic profiling

<b>SUPPLEMENTARY NOTE TABLES</b>	<b>2</b>
Supplementary Note Table 1: Patient characteristics by cohort.	2
Supplementary Note Table 2: Patient characteristics by genotyping subcohort.	4
Supplementary Note Table 3: Patient characteristics by treatment centre.	6
Supplementary Note Table 4: Patient characteristics by genetic subtype.	10
<b>SUPPLEMENTARY NOTE FIGURES</b>	<b>11</b>
Supplementary Note Figure 1: Comparison of SNV calls in matched Plasma and Tumour specimens.	11
Supplementary Note Figure 2: Mutation enrichment through laser microdissection (LMD).	12
Supplementary Note Figure 3: Cancer cell fractions in large B-cell lymphoma (LBCL) and classic Hodgkin lymphoma (cHL).	13
Supplementary Note Figure 4: Bulk <i>DNASE1L3</i> expression in cHL and LBCL.	14
Supplementary Note Figure 5: <i>DNASE1L3</i> bulk tissue expression.	15
Supplementary Note Figure 6: <i>DNASE1L3</i> tumour bulk expression relative to normal tissue.	16
Supplementary Note Figure 7: Single-cell RNA-Sequencing.	17
Supplementary Note Figure 8: Mutation frequencies in the exome cohort (n=119) as compared to the full genotyping cohort (n=293).	18
Supplementary Note Figure 9: Lollipop plots of significantly mutated genes.	19
Supplementary Note Figure 10: Raw cell line flow data.	26
Supplementary Note Figure 11: Bulk <i>IL13</i> and <i>IL4</i> expression by histology.	32
Supplementary Note Figure 12: <i>IL13</i> and <i>IL4</i> expression by histology in public datasets.	33
Supplementary Note Figure 13: Recursive Phylon Nomination, Enumeration, and Recovery (RePhyNER) to allow for reliable germline-free MRD detection.	34
Supplementary Note Figure 14: Pre-sorting gates prior to scRNA-Sequencing.	35
Supplementary Note Figure 15: PhosphoSTAT6 flow gates.	36
Supplementary Note Figure 16: Full immunoblot scans.	37
<b>REFERENCES</b>	<b>42</b>

**SUPPLEMENTARY NOTE TABLES**

**Supplementary Note Table 1: Patient characteristics by cohort.**

	<b>Plasma cohort, N = 366<sup>1</sup></b>	<b>Genotyping cohort, N = 293<sup>1</sup></b>	<b>MRD cohort, N = 109<sup>1</sup></b>
<b>Age</b>	32 (4-88)	31 (7-88)	29 (18-78)
<b>Male sex</b>	191 / 352 (54%)	157 / 288 (55%)	54 / 109 (50%)
<b>EBV positivity</b>	91 / 366 (25%)	72 / 293 (25%)	14 / 109 (13%)
<b>Stage</b>			
I/II	183 / 351 (52%)	142 / 287 (49%)	76 / 109 (70%)
favourable risk	15 / 166 (9.0%)	5 / 129 (3.9%)	1 / 76 (1.3%)
unfavourable risk	151 / 166 (91%)	124 / 129 (96%)	75 / 76 (99%)
III/IV	168 / 351 (48%)	145 / 287 (51%)	33 / 109 (30%)
<b>Histological subtype</b>			
NS	242 / 295 (82%)	204 / 241 (85%)	73 / 80 (91%)
MC	43 / 295 (15%)	32 / 241 (13%)	5 / 80 (6.2%)
LR	8 / 295 (2.7%)	3 / 241 (1.2%)	2 / 80 (2.5%)
LD	2 / 295 (0.7%)	2 / 241 (0.8%)	0 / 80 (0%)

<sup>1</sup>Median (Minimum-Maximum); n / N (%); Favourable/unfavourable risk profile of patients with stage I/II disease is not reported for paediatric cohorts.

**Supplementary Note Table 1: Patient characteristics by cohort (continued).**

	Plasma cohort, N = 366 <sup>1</sup>	Genotyping cohort, N = 293 <sup>1</sup>	MRD cohort, N = 109 <sup>1</sup>
<b>Cohort</b>			
AHL2011 trial, FR/BE	40 / 366 (11%)	34 / 293 (12%)	0 / 109 (0%)
Bellinzona, CH	30 / 366 (8.2%)	23 / 293 (7.8%)	9 / 109 (8.3%)
BREACH trial, FR/BE	102 / 366 (28%)	86 / 293 (29%)	61 / 109 (56%)
Leuven, BE	29 / 366 (7.9%)	20 / 293 (6.8%)	8 / 109 (7.3%)
PAVD trial, WA	30 / 366 (8.2%)	25 / 293 (8.5%)	25 / 109 (23%)
Paediatric studies, USA	44 / 366 (12%)	30 / 293 (10%)	0 / 109 (0%)
PVAB trial, FR/BE	58 / 366 (16%)	48 / 293 (16%)	0 / 109 (0%)
Stanford, CA	33 / 366 (9.0%)	27 / 293 (9.2%)	6 / 109 (5.5%)
<b>Therapy</b>			
ABVD	86 / 366 (23%)	65 / 293 (22%)	25 / 109 (23%)
BEACOPP	49 / 366 (13%)	41 / 293 (14%)	4 / 109 (3.7%)
BRECADD	4 / 366 (1.1%)	4 / 293 (1.4%)	3 / 109 (2.8%)
Bv-AVD	73 / 366 (20%)	62 / 293 (21%)	50 / 109 (46%)
Bv-Nivolumab	4 / 366 (1.1%)	3 / 293 (1.0%)	1 / 109 (0.9%)
Bv-Nivolumab- Ipilimumab	1 / 366 (0.3%)	1 / 293 (0.3%)	0 / 109 (0%)
Other conventional chemotherapy	7 / 366 (1.9%)	5 / 293 (1.7%)	0 / 109 (0%)
PAVD	30 / 366 (8.2%)	25 / 293 (8.5%)	25 / 109 (23%)
Paediatric regimens	44 / 366 (12%)	30 / 293 (10%)	0 / 109 (0%)
Pembrolizumab-AVD	3 / 366 (0.8%)	3 / 293 (1.0%)	1 / 109 (0.9%)
PVAB	58 / 366 (16%)	48 / 293 (16%)	0 / 109 (0%)
Stanford V	7 / 366 (1.9%)	6 / 293 (2.0%)	0 / 109 (0%)

<sup>1</sup>n / N (%); The starting therapy regimen is summarized in this table. Escalation/de-escalation is not considered (*e.g.* de-escalation from ABVD to AVD after negative PET2 is reported as ABVD, as are cases where therapy was escalated from ABVD to BEACOPP).

**Supplementary Note Table 2: Patient characteristics by genotyping subcohort.**

	<b>Genotyping cohort,</b> N = 293 <sup>1</sup>	<b>Exome cohort,</b> N = 119 <sup>1</sup>	<b>EPIC cohort,</b> N = 113 <sup>1</sup>
<b>Age</b>	31 (7-88)	24 (8-78)	31 (8-80)
<b>Male sex</b>	157 / 288 (55%)	56 / 116 (48%)	67 / 111 (60%)
<b>EBV positivity</b>	72 / 293 (25%)	23 / 119 (19%)	27 / 113 (24%)
<b>Stage</b>			
I/II	142 / 287 (49%)	83 / 116 (72%)	51 / 111 (46%)
favourable risk	5 / 129 (3.9%)	2 / 75 (2.7%)	2 / 47 (4.3%)
unfavourable risk	124 / 129 (96%)	73 / 75 (97%)	45 / 47 (96%)
III/IV	145 / 287 (51%)	33 / 116 (28%)	60 / 111 (54%)
<b>Histological subtype</b>			
NS	204 / 241 (85%)	91 / 100 (91%)	82 / 95 (86%)
MC	32 / 241 (13%)	8 / 100 (8.0%)	10 / 95 (11%)
LR	3 / 241 (1.2%)	1 / 100 (1.0%)	1 / 95 (1.1%)
LD	2 / 241 (0.8%)	0 / 100 (0%)	2 / 95 (2.1%)

<sup>1</sup>Median (Minimum-Maximum); n / N (%); Favourable/unfavourable risk profile of patients with stage I/II disease is not reported for paediatric cohorts.

**Supplementary Note Table 2: Patient characteristics by genotyping subcohort (continued).**

	Genotyping cohort, N = 293 <sup>1</sup>	Exome cohort, N = 119 <sup>1</sup>	EPIC cohort, N = 113 <sup>1</sup>
<b>Cohort</b>			
AHL2011 trial, FR/BE	34 / 293 (12%)	0 / 119 (0%)	10 / 113 (8.8%)
Bellinzona, CH	23 / 293 (7.8%)	5 / 119 (4.2%)	7 / 113 (6.2%)
BREACH trial, FR/BE	86 / 293 (29%)	59 / 119 (50%)	35 / 113 (31%)
Leuven, BE	20 / 293 (6.8%)	13 / 119 (11%)	4 / 113 (3.5%)
PAVD trial, WA	25 / 293 (8.5%)	7 / 119 (5.9%)	7 / 113 (6.2%)
Paediatric studies, USA	30 / 293 (10%)	21 / 119 (18%)	12 / 113 (11%)
PVAB trial, FR/BE	48 / 293 (16%)	0 / 119 (0%)	24 / 113 (21%)
Stanford, CA	27 / 293 (9.2%)	14 / 119 (12%)	14 / 113 (12%)
<b>Therapy</b>			
ABVD	65 / 293 (22%)	39 / 119 (33%)	25 / 113 (22%)
BEACOPP	41 / 293 (14%)	2 / 119 (1.7%)	14 / 113 (12%)
BRECADD	4 / 293 (1.4%)	1 / 119 (0.8%)	0 / 113 (0%)
Bv-AVD	62 / 293 (21%)	41 / 119 (34%)	26 / 113 (23%)
Bv-Nivolumab	3 / 293 (1.0%)	1 / 119 (0.8%)	0 / 113 (0%)
Bv-Nivolumab- Ipilimumab	1 / 293 (0.3%)	0 / 119 (0%)	0 / 113 (0%)
Other conventional chemotherapy	5 / 293 (1.7%)	2 / 119 (1.7%)	1 / 113 (0.9%)
PAVD	25 / 293 (8.5%)	7 / 119 (5.9%)	7 / 113 (6.2%)
Paediatric regimens	30 / 293 (10%)	21 / 119 (18%)	12 / 113 (11%)
Pembrolizumab-AVD	3 / 293 (1.0%)	1 / 119 (0.8%)	1 / 113 (0.9%)
PVAB	48 / 293 (16%)	0 / 119 (0%)	24 / 113 (21%)
Stanford V	6 / 293 (2.0%)	4 / 119 (3.4%)	3 / 113 (2.7%)

<sup>1</sup>n / N (%); The starting therapy regimen is summarized in this table. Escalation/de-escalation is not considered (*e.g.* de-escalation from ABVD to AVD after negative PET2 is reported as ABVD, as are cases where therapy was escalated from ABVD to BEACOPP).

**Supplementary Note Table 3: Patient characteristics by treatment centre.**

	<b>AHL2011 trial, FR/BE, N = 40<sup>1</sup></b>	<b>Bellinzona, CH, N = 30<sup>1</sup></b>	<b>BREACH trial, FR/BE, N = 102<sup>1</sup></b>	<b>Leuven, BE, N = 29<sup>1</sup></b>	<b>PAVD trial, WA, N = 30<sup>1</sup></b>	<b>Paediatric studies, USA, N = 44<sup>1</sup></b>	<b>PVAB trial, FR/BE, N = 58<sup>1</sup></b>	<b>Stanford, CA, N = 33<sup>1</sup></b>
<b>Age</b>	33 (17-60)	38 (16-78)	28 (18-60)	28 (12-86)	32 (18-69)	14 (4-20)	68 (61-88)	32 (17-79)
<b>Male sex</b>	29 / 40 (72%)	16 / 30 (53%)	50 / 102 (49%)	11 / 29 (38%)	12 / 30 (40%)	16 / 30 (53%)	39 / 58 (67%)	18 / 33 (55%)
<b>EBV positivity</b>	14 / 40 (35%)	10 / 30 (33%)	8 / 102 (7.8%)	7 / 29 (24%)	5 / 30 (17%)	19 / 44 (43%)	22 / 58 (38%)	6 / 33 (18%)
<b>Stage</b>								
I/II	5 / 40 (12%)	13 / 30 (43%)	101 / 102 (99%)	14 / 29 (48%)	12 / 30 (40%)	17 / 29 (59%)	1 / 58 (1.7%)	20 / 33 (61%)
Favourable risk	0 / 5 (0%)	4 / 13 (31%)	0 / 101 (0%)	5 / 14 (36%)	2 / 12 (17%)	0 / 0 (NA%)	0 / 1 (0%)	4 / 20 (20%)
Unfavourable risk	5 / 5 (100%)	9 / 13 (69%)	101 / 101 (100%)	9 / 14 (64%)	10 / 12 (83%)	0 / 0 (NA%)	1 / 1 (100%)	16 / 20 (80%)
III/IV	35 / 40 (88%)	17 / 30 (57%)	1 / 102 (1.0%)	15 / 29 (52%)	18 / 30 (60%)	12 / 29 (41%)	57 / 58 (98%)	13 / 33 (39%)

<sup>1</sup>Median (Minimum-Maximum); n / N (%); Favourable/unfavourable risk profile of patients with stage I/II disease is not reported for paediatric cohorts.

**Supplementary Note Table 3: Patient characteristics by treatment centre (continued).**

	<b>AHL2011 trial, FR/BE, N = 40<sup>1</sup></b>	<b>Bellinzona, CH, N = 30<sup>1</sup></b>	<b>BREACH trial, FR/BE, N = 102<sup>1</sup></b>	<b>Leuven, BE, N = 29<sup>1</sup></b>	<b>PAVD trial, WA, N = 30<sup>1</sup></b>	<b>Paediatric studies, USA, N = 44<sup>1</sup></b>	<b>PVAB trial, FR/BE, N = 58<sup>1</sup></b>	<b>Stanford, CA, N = 33<sup>1</sup></b>
<b>Histological subtype</b>								
NS	33 / 39 (85%)	17 / 28 (61%)	92 / 98 (94%)	16 / 26 (62%)	0 / 0 (NA%)	22 / 27 (81%)	41 / 51 (80%)	21 / 26 (81%)
MC	4 / 39 (10%)	11 / 28 (39%)	5 / 98 (5.1%)	5 / 26 (19%)	0 / 0 (NA%)	5 / 27 (19%)	8 / 51 (16%)	5 / 26 (19%)
LR	1 / 39 (2.6%)	0 / 28 (0%)	1 / 98 (1.0%)	4 / 26 (15%)	0 / 0 (NA%)	0 / 27 (0%)	2 / 51 (3.9%)	0 / 26 (0%)
LD	1 / 39 (2.6%)	0 / 28 (0%)	0 / 98 (0%)	1 / 26 (3.8%)	0 / 0 (NA%)	0 / 27 (0%)	0 / 51 (0%)	0 / 26 (0%)
<b>Genotyping cohort</b>	34 / 40 (85%)	23 / 30 (77%)	86 / 102 (84%)	20 / 29 (69%)	25 / 30 (83%)	30 / 44 (68%)	48 / 58 (83%)	27 / 33 (82%)
<b>EPIC cohort</b>	10 / 40 (25%)	7 / 30 (23%)	35 / 102 (34%)	4 / 29 (14%)	7 / 30 (23%)	12 / 44 (27%)	24 / 58 (41%)	14 / 33 (42%)
<b>Exome cohort</b>	0 / 40 (0%)	5 / 30 (17%)	59 / 102 (58%)	13 / 29 (45%)	7 / 30 (23%)	21 / 44 (48%)	0 / 58 (0%)	14 / 33 (42%)
<b>MRD cohort</b>	0 / 40 (0%)	9 / 30 (30%)	61 / 102 (60%)	8 / 29 (28%)	25 / 30 (83%)	0 / 44 (0%)	0 / 58 (0%)	6 / 33 (18%)

<sup>1</sup>n / N (%)

**Supplementary Note Table 3: Patient characteristics by treatment centre (continued).**

	AHL2011 trial, FR/BE, N = 40 <sup>1</sup>	Bellinzona, CH, N = 30 <sup>1</sup>	BREACH trial, FR/BE, N = 102 <sup>1</sup>	Leuven, BE, N = 29 <sup>1</sup>	PAVD trial, WA, N = 30 <sup>1</sup>	Paediatric studies, USA, N = 44 <sup>1</sup>	PVAB trial, FR/BE, N = 58 <sup>1</sup>	Stanford, CA, N = 33 <sup>1</sup>
<b>Therapy</b>								
ABVD	0 / 40 (0%)	18 / 30 (60%)	35 / 102 (34%)	23 / 29 (79%)	0 / 30 (0%)	0 / 44 (0%)	0 / 58 (0%)	10 / 33 (30%)
BEACOPP	40 / 40 (100%)	8 / 30 (27%)	0 / 102 (0%)	0 / 29 (0%)	0 / 30 (0%)	0 / 44 (0%)	0 / 58 (0%)	1 / 33 (3.0%)
BRECADD	0 / 40 (0%)	4 / 30 (13%)	0 / 102 (0%)	0 / 29 (0%)	0 / 30 (0%)	0 / 44 (0%)	0 / 58 (0%)	0 / 33 (0%)
Bv-AVD	0 / 40 (0%)	0 / 30 (0%)	67 / 102 (66%)	0 / 29 (0%)	0 / 30 (0%)	0 / 44 (0%)	0 / 58 (0%)	6 / 33 (18%)
Bv-Nivolumab	0 / 40 (0%)	0 / 30 (0%)	0 / 102 (0%)	0 / 29 (0%)	0 / 30 (0%)	0 / 44 (0%)	0 / 58 (0%)	4 / 33 (12%)
Bv-Nivolumab- Ipilimumab	0 / 40 (0%)	0 / 30 (0%)	0 / 102 (0%)	0 / 29 (0%)	0 / 30 (0%)	0 / 44 (0%)	0 / 58 (0%)	1 / 33 (3.0%)
Other conventional chemotherapy	0 / 40 (0%)	0 / 30 (0%)	0 / 102 (0%)	6 / 29 (21%)	0 / 30 (0%)	0 / 44 (0%)	0 / 58 (0%)	1 / 33 (3.0%)
PAVD	0 / 40 (0%)	0 / 30 (0%)	0 / 102 (0%)	0 / 29 (0%)	30 / 30 (100%)	0 / 44 (0%)	0 / 58 (0%)	0 / 33 (0%)
Paediatric regimens	0 / 40 (0%)	0 / 30 (0%)	0 / 102 (0%)	0 / 29 (0%)	0 / 30 (0%)	44 / 44 (100%)	0 / 58 (0%)	0 / 33 (0%)

<sup>1</sup>n / N (%); The starting therapy regimen is summarized in this table. Escalation/de-escalation is not considered (*e.g.* de-escalation from ABVD to AVD after negative PET2 is reported as ABVD, as are cases where therapy was escalated from ABVD to BEACOPP).

**Supplementary Note Table 3: Patient characteristics by treatment centre (continued).**

	AHL2011 trial, FR/BE, N = 40 <sup>1</sup>	Bellinzona, CH, N = 30 <sup>1</sup>	BREACH trial, FR/BE, N = 102 <sup>1</sup>	Leuven, BE, N = 29 <sup>1</sup>	PAVD trial, WA, N = 30 <sup>1</sup>	Paediatric studies, USA, N = 44 <sup>1</sup>	PVAB trial, FR/BE, N = 58 <sup>1</sup>	Stanford, CA, N = 33 <sup>1</sup>
<b>Therapy (continued)</b>								
Pembrolizumab -AVD	0 / 40 (0%)	0 / 30 (0%)	0 / 102 (0%)	0 / 29 (0%)	0 / 30 (0%)	0 / 44 (0%)	0 / 58 (0%)	3 / 33 (9.1%)
PVAB	0 / 40 (0%)	0 / 30 (0%)	0 / 102 (0%)	0 / 29 (0%)	0 / 30 (0%)	0 / 44 (0%)	58 / 58 (100%)	0 / 33 (0%)
Stanford V	0 / 40 (0%)	0 / 30 (0%)	0 / 102 (0%)	0 / 29 (0%)	0 / 30 (0%)	0 / 44 (0%)	0 / 58 (0%)	7 / 33 (21%)

<sup>1</sup>n / N (%); The starting therapy regimen is summarized in this table. Escalation/de-escalation is not considered (*e.g.* de-escalation from ABVD to AVD after negative PET2 is reported as ABVD, as are cases where therapy was escalated from ABVD to BEACOPP).

**Supplementary Note Table 4: Patient characteristics by genetic subtype.**

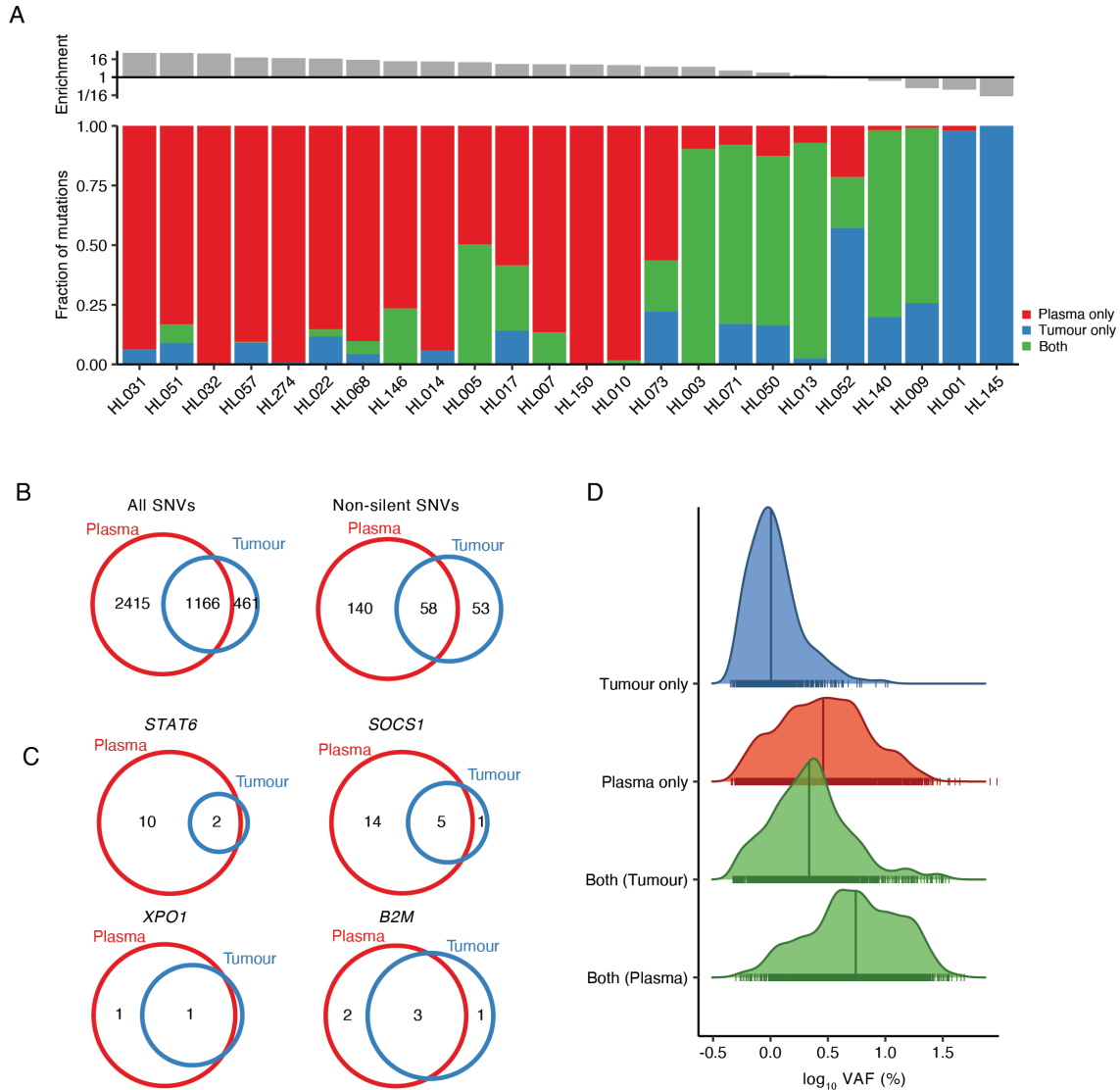
	H1, N = 200 <sup>1</sup>	H2, N = 93 <sup>1</sup>	P-value <sup>2</sup>
<b>Age</b>	30 (7-78)	42 (8-88)	0.021
<b>Male sex</b>	98 / 199 (49%)	59 / 89 (66%)	0.007
<b>EBV positivity</b>	35 / 200 (18%)	37 / 93 (40%)	6.9 x 10 <sup>-5</sup>
<b>TMTV</b>	143 (7-2,235)	198 (19-1,861)	0.012
<b>B-symptoms</b>	99 / 197 (50%)	56 / 89 (63%)	0.055
<b>Mediastinal Mass</b>	102 / 184 (55%)	32 / 77 (42%)	0.043
<b>Stage</b>			4.3 x 10 <sup>-5</sup>
I/II	114 / 198 (58%)	28 / 89 (31%)	
favourable risk	3 / 111 (2.7%)	2 / 18 (11%)	
unfavourable risk	108 / 111 (97%)	16 / 18 (89%)	
III/IV	84 / 198 (42%)	61 / 89 (69%)	
<b>Histological subtype</b>			0.010
NS	150 / 168 (89%)	54 / 73 (74%)	
MC	15 / 168 (8.9%)	17 / 73 (23%)	
LR	2 / 168 (1.2%)	1 / 73 (1.4%)	
LD	1 / 168 (0.6%)	1 / 73 (1.4%)	

<sup>1</sup>Median (Minimum-Maximum); n / N (%)

<sup>2</sup>Wilcoxon rank sum test; Fisher's exact test (two-sided)

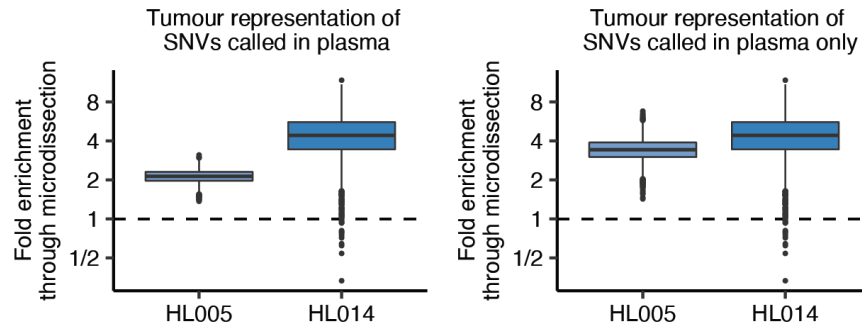
**SUPPLEMENTARY NOTE FIGURES**

**Supplementary Note Figure 1: Comparison of SNV calls in matched Plasma and Tumour specimens.**



(A) Stacked bar plot visualizing the fractions of SNVs called in Plasma, Tumour, or Both in 24 patients with matched specimens. Patients are ordered by plasma enrichment of mutations (top annotation) as shown in Fig. 1B. (B) Venn Diagrams visualizing all SNVs called in plasma and/or tumour specimens, and separately for the subset of non-silent SNVs. (C) Venn Diagrams visualizing non-silent mutations in canonical cHL genes called in Plasma and/or Tumour specimens. (D) Comparison of VAFs of SNVs called in plasma and/or tumour samples visualized by density ridge plots. Notably, median VAF of mutations only called in Tumour tissue was <1% suggestive of enrichment for artifacts due to tissue fixation. VAF: variant allelic fraction; SNV: single nucleotide variants.

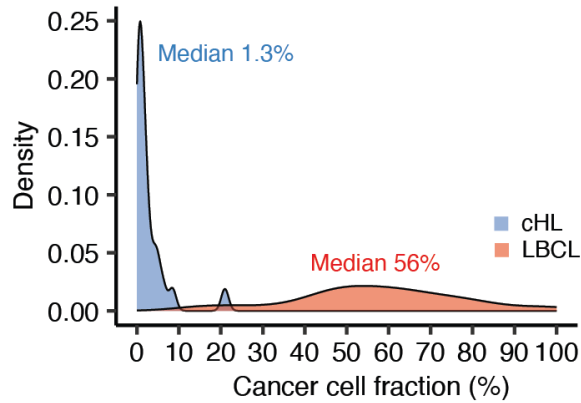
**Supplementary Note Figure 2: Mutation enrichment through laser microdissection (LMD).**



Boxplots summarize the enrichment of SNVs called in 2 plasma samples (HL005 and HL014) through laser microdissection (LMD) in 5,000 bootstrap iterations. SNVs called in plasma samples (left, HL005: n=226; HL014: n=63) as well as the subset of plasma SNVs not called in the tumour (right, HL005: n=113; HL014: n=63) were sampled with replacement recording the mean AF across all sampled variants prior to and post LMD for each iteration. Boxplots visualize the enrichment in mean AF through LMD across the sampling iterations.

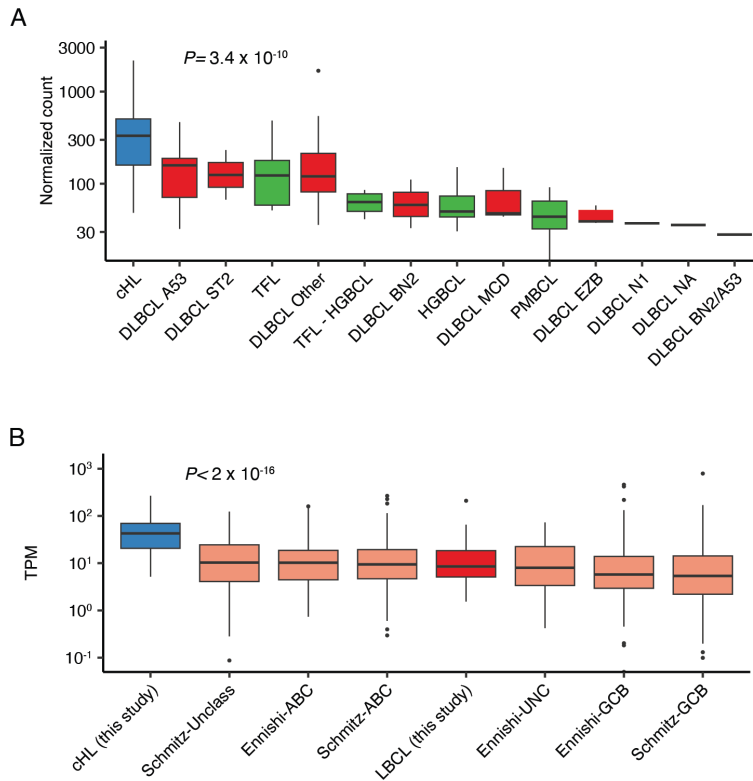
*Each box represents the interquartile range (the range between the 25th and 75th percentile) with the median of the data, whiskers indicate the upper and lower value within 1.5 times the IQR.*

**Supplementary Note Figure 3: Cancer cell fractions in large B-cell lymphoma (LBCL) and classic Hodgkin lymphoma (cHL).**



Cancer cell fractions were estimated from mutation calls as  $2 * \text{mean allele fraction (AF)}$  assuming heterozygous mutation states. LBCL (n=63) AFs were calculated from bona fide tumour mutation calls. In cHL (n=24), the mean tumour AF was calculated by monitoring for variants called in either tumour or matched plasma specimen.

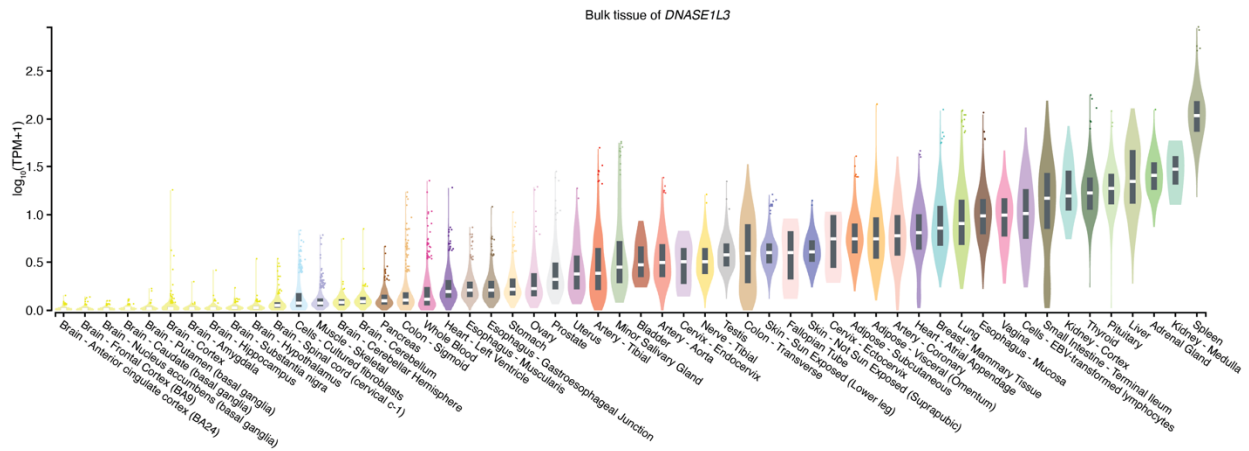
**Supplementary Note Figure 4: Bulk *DNASE1L3* expression in cHL and LBCL.**



**(A)** Boxplot comparing *DNASE1L3* expression assessed within this study by bulk RNA-Sequencing visualized as normalized counts by histology and genetic subtype. Kruskal-Wallis p-value is provided. Subtypes with  $n < 3$  were excluded from statistical testing. Classic Hodgkin Lymphoma (cHL),  $n=86$ ; Diffuse Large B-cell Lymphoma (DLBCL) A53,  $n=8$ ; DLBCL ST2,  $n=2$ ; Transformed Follicular Lymphoma (TFL),  $n=13$ ; DLBCL Other,  $n=12$ ; TFL-High-grade B-cell Lymphoma (HGBCL),  $n=4$ ; DLBCL BN2,  $n=3$ ; HGBCL,  $n=8$ ; DLBCL MCD,  $n=3$ ; Primary Mediastinal B-cell lymphoma (PMBL),  $n=5$ ; DLBCL EZB,  $n=5$ ; DLBCL N1,  $n=1$ ; DLBCL NOS,  $n=1$ ; DLBCL BN2/A53,  $n=1$ . **(B)** *DNASE1L3* expression assessed within this study put in context with publicly available datasets. TPM values for overlapping genes reported across datasets were renormalized and visualized. Datasets from Schmitz, *NEJM* 2018<sup>1</sup> and Ennishi, *Journal of Clin Oncol* 2019<sup>2</sup> were used for the analysis. Kruskal-Wallis p-value is provided. cHL (this study):  $n=86$ ; LBCL (this study):  $n=66$ ; Ennishi-ABC:  $n=93$ ; Ennishi-GCB:  $n=168$ ; Ennishi-UNC:  $n=33$ ; Schmitz-ABC:  $n=243$ ; Schmitz-GCB:  $n=138$ ; Schmitz-UNC:  $n=100$ .

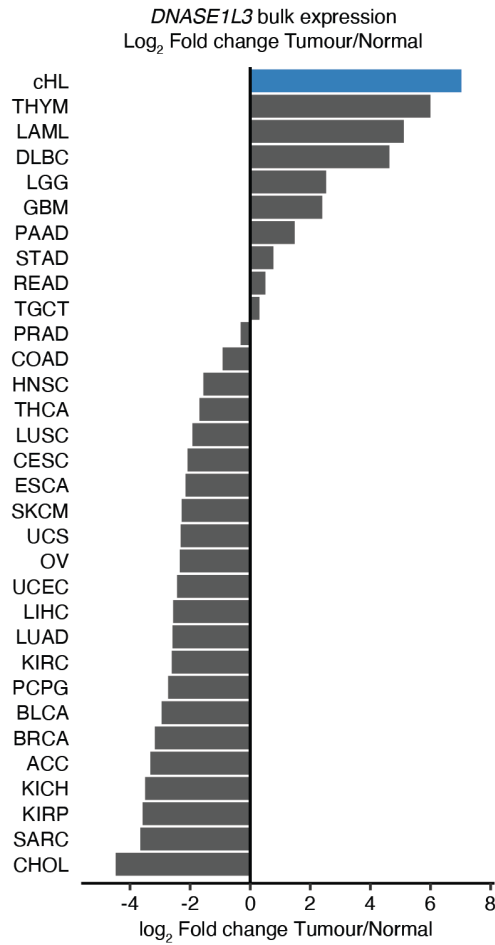
Each box represents the interquartile range (the range between the 25th and 75th percentile) with the median of the data, whiskers indicate the upper and lower value within 1.5 times the IQR.

Supplementary Note Figure 5: *DNASE1L3* bulk tissue expression.



Tissue expression of *DNASE1L3* according to GTEx Portal (<https://www.gtexportal.org>) sorted from low to high expressed as log<sub>10</sub> Transcripts per million (TPM).

**Supplementary Note Figure 6: *DNASE1L3* tumour bulk expression relative to normal tissue.**

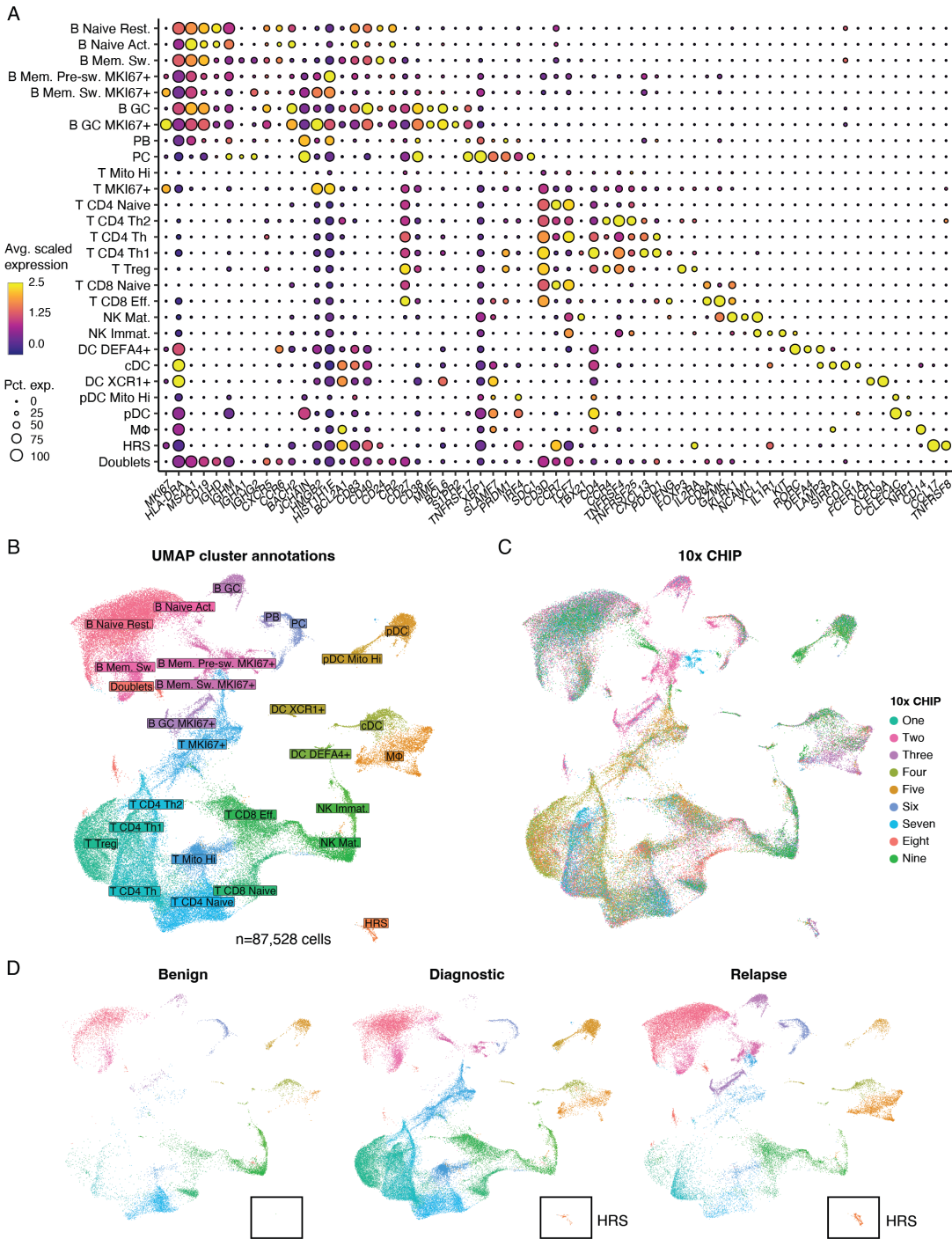


*DNASE1L3* Tumour bulk expression relative to matched normal tissue in cHL (this study) and 31 other cancers according to GEPIA (<http://gepia.cancer-pku.cn>). Median TPMs for each Tumour/Normal pair were downloaded from GEPIA, and expressed as log<sub>2</sub> fold change Tumour/Normal. For cHL, the median TPM was normalized to DLBC analysed as part of this study, and the DLBC normal tissue from GEPIA was used as denominator.

cHL: Classic Hodgkin Lymphoma; THYM: Thymoma; LAML: Acute Myeloid Leukaemia; DLBC: Lymphoid Neoplasm Diffuse Large B-cell Lymphoma; LGG: Brain Lower Grade Glioma; GBM: Glioblastoma multiforme; PAAD: Pancreatic adenocarcinoma; STAD: Stomach adenocarcinoma; READ: Rectum adenocarcinoma; TGCT: Testicular Germ Cell Tumours; PRAD: Prostate adenocarcinoma; COAD: Colon adenocarcinoma; HNSC: Head and Neck squamous cell carcinoma; THCA: Thyroid carcinoma; LUSC: Lung squamous cell carcinoma; CESC: Cervical squamous cell carcinoma; ESCA: Oesophageal carcinoma; SKCM: Skin Cutaneous Melanoma; UCS: Uterine Carcinosarcoma; OV: Ovarian serous cystadenocarcinoma; UCEC: Uterine Corpus Endometrial Carcinoma; LIHC: Liver hepatocellular carcinoma; LUAD: Lung adenocarcinoma; KIRC: Kidney renal clear cell carcinoma; PCPG: Pheochromocytoma and Paraganglioma; BLCA: Bladder Urothelial Carcinoma; BRCA: Breast invasive carcinoma; ACC: Adrenocortical carcinoma; KICH: Kidney Chromophobe; KIRP: Kidney renal papillary cell carcinoma; SARC: Sarcoma; CHOL: Cholangiocarcinoma.

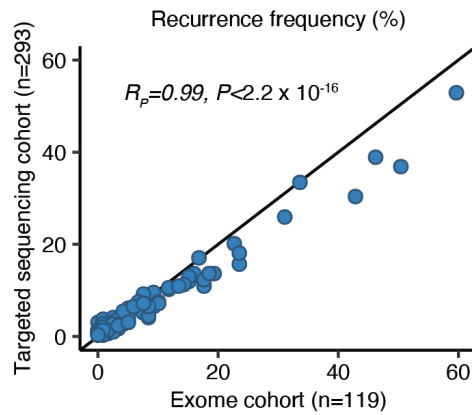
Cervical squamous cell carcinoma and endocervical adenocarcinoma; ESCA: Oesophageal carcinoma; SKCM: Skin Cutaneous Melanoma; UCS: Uterine Carcinosarcoma; OV: Ovarian serous cystadenocarcinoma; UCEC: Uterine Corpus Endometrial Carcinoma; LIHC: Liver hepatocellular carcinoma; LUAD: Lung adenocarcinoma; KIRC: Kidney renal clear cell carcinoma; PCPG: Pheochromocytoma and Paraganglioma; BLCA: Bladder Urothelial Carcinoma; BRCA: Breast invasive carcinoma; ACC: Adrenocortical carcinoma; KICH: Kidney Chromophobe; KIRP: Kidney renal papillary cell carcinoma; SARC: Sarcoma; CHOL: Cholangiocarcinoma.

Supplementary Note Figure 7: Single-cell RNA-Sequencing.



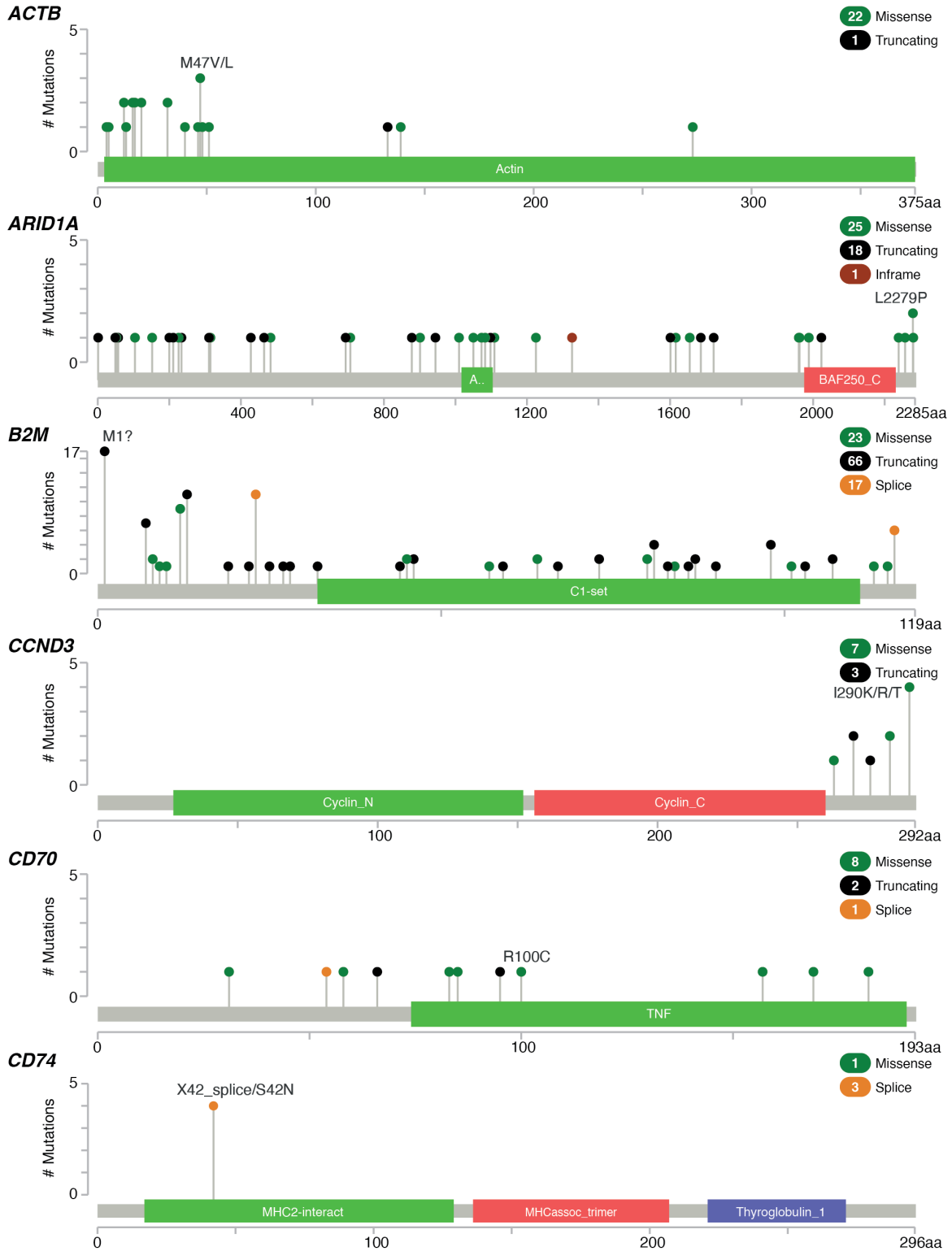
(A) Dotplot summarizing expression of key marker genes supporting UMAP cluster annotations. Heat denotes average (Avg.) scaled expression, while size depicts percent expression (Pct. exp.). (B) Uniform manifold approximation and projection (UMAP) depiction of single-cell clusters with their respective annotation. Dots are coloured by UMAP cluster. A total of n=87,528 cells were included in the analysis. (C) UMAP visualization of single-cell clusters by 10x CHIP used for library preparation (colour). (D) UMAP visualization of single-cells broken up by cells profiled from benign lymph-nodes (left), initial diagnosis of cHL (middle) and relapse of cHL (right).

**Supplementary Note Figure 8: Mutation frequencies in the exome cohort (n=119) as compared to the full genotyping cohort (n=293).**

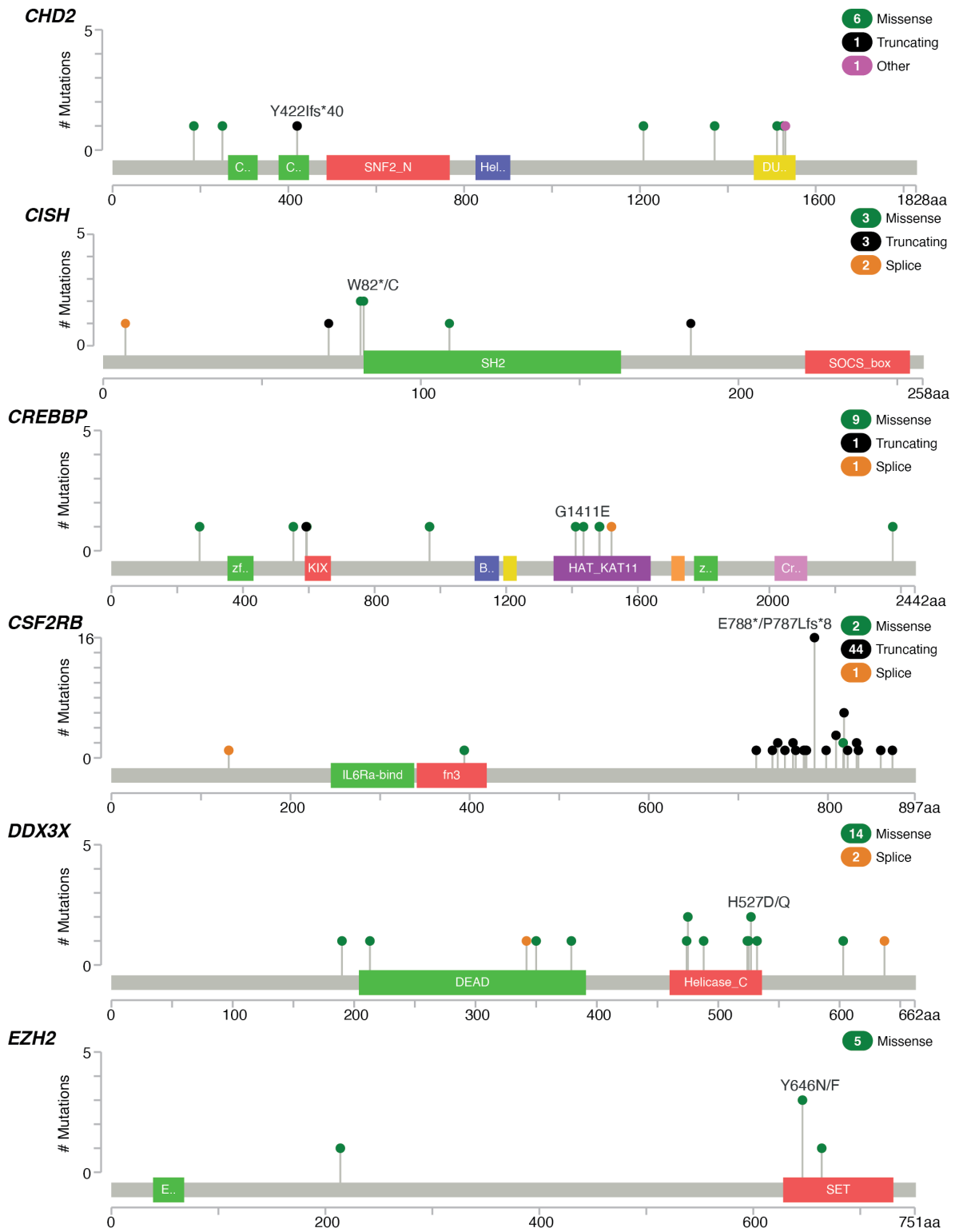


Gene mutation recurrence frequencies in the exome cohort (n=119) as compared to the full genotyping cohort (n=293). Each dot represents a gene fully targeted in the CAPP-Seq panel. Pearson correlation coefficient and corresponding p-value (asymptotic approximation) are provided in the graph.

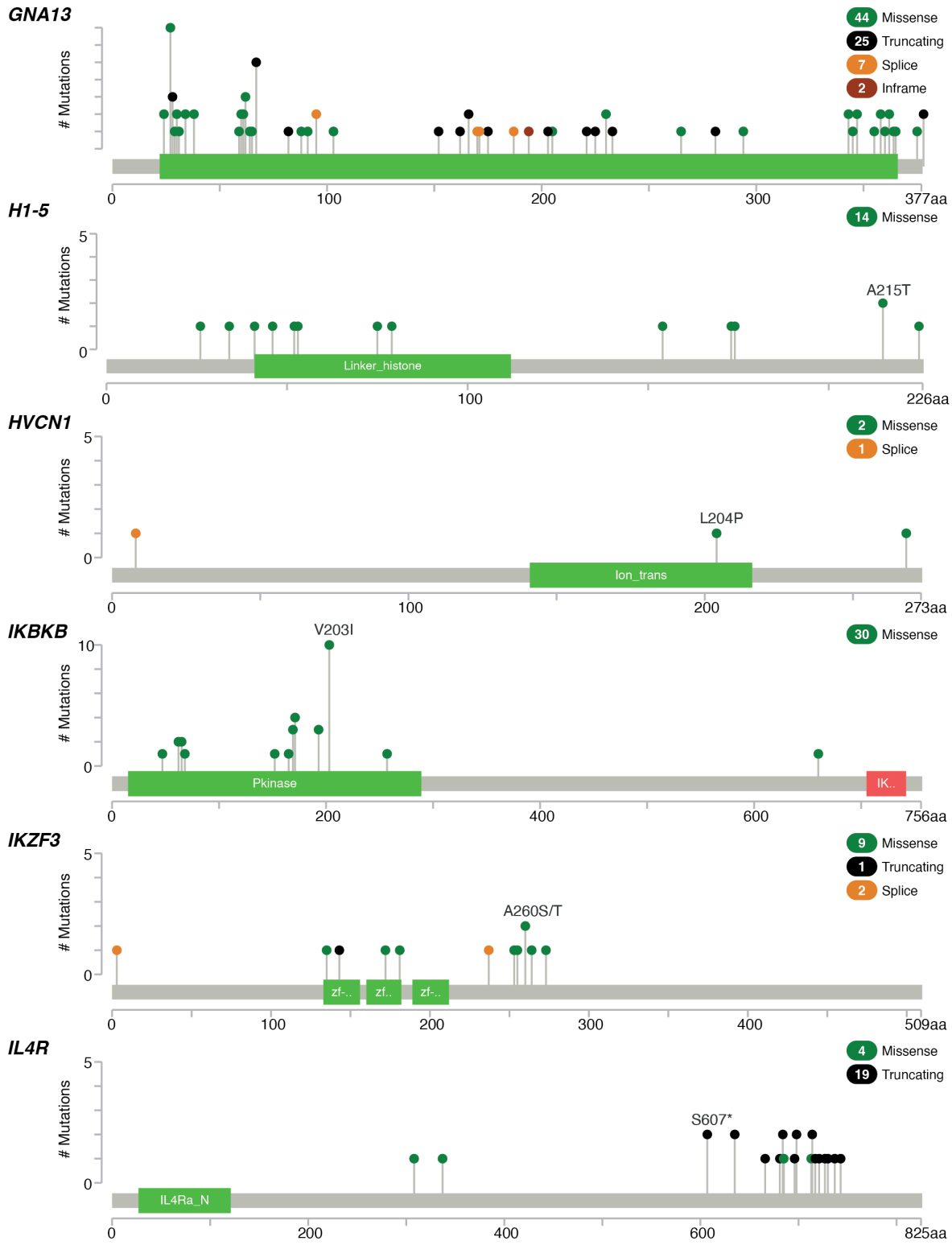
Supplementary Note Figure 9: Lollipop plots of significantly mutated genes.



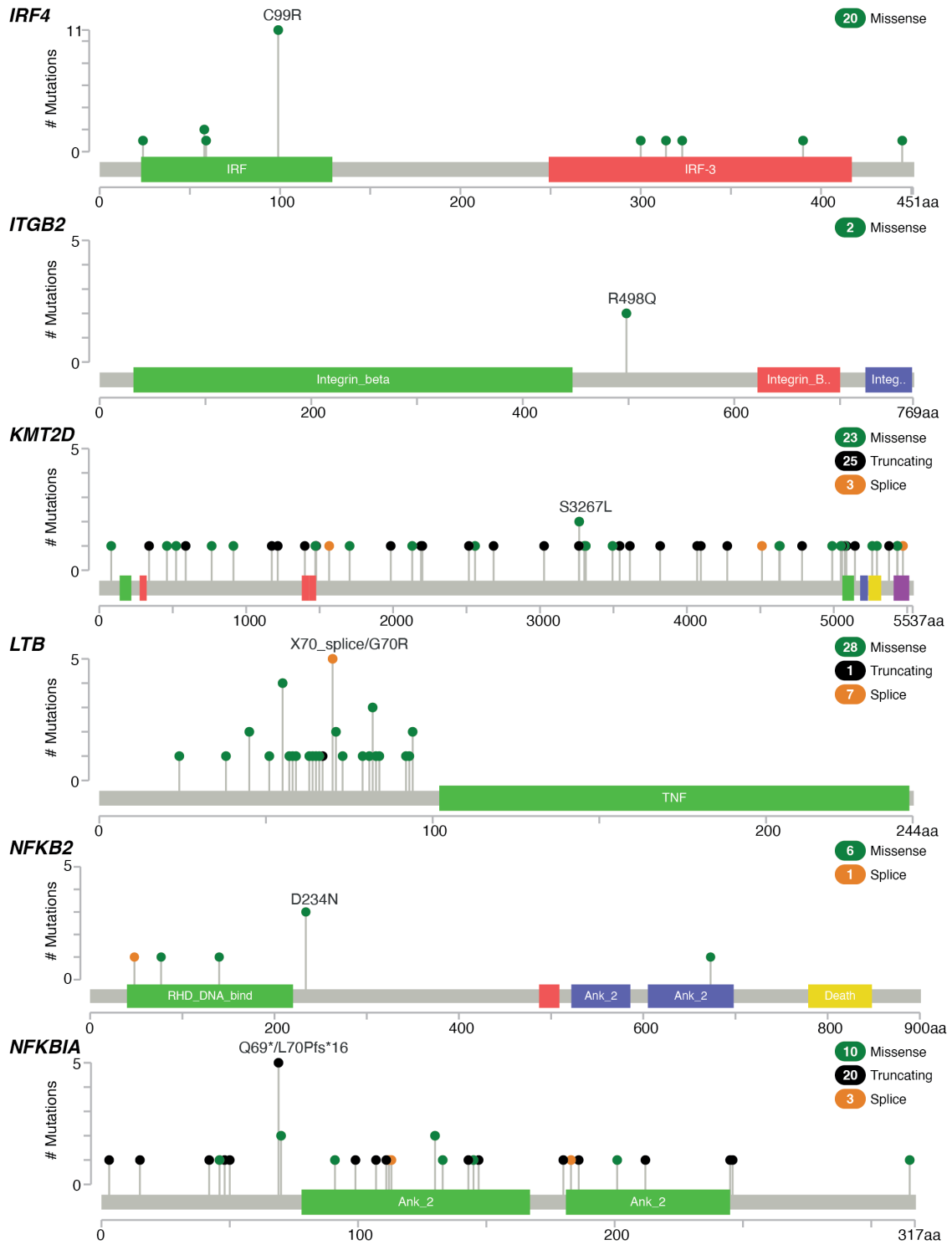
Alig S. *et al.*, ctDNA in cHL



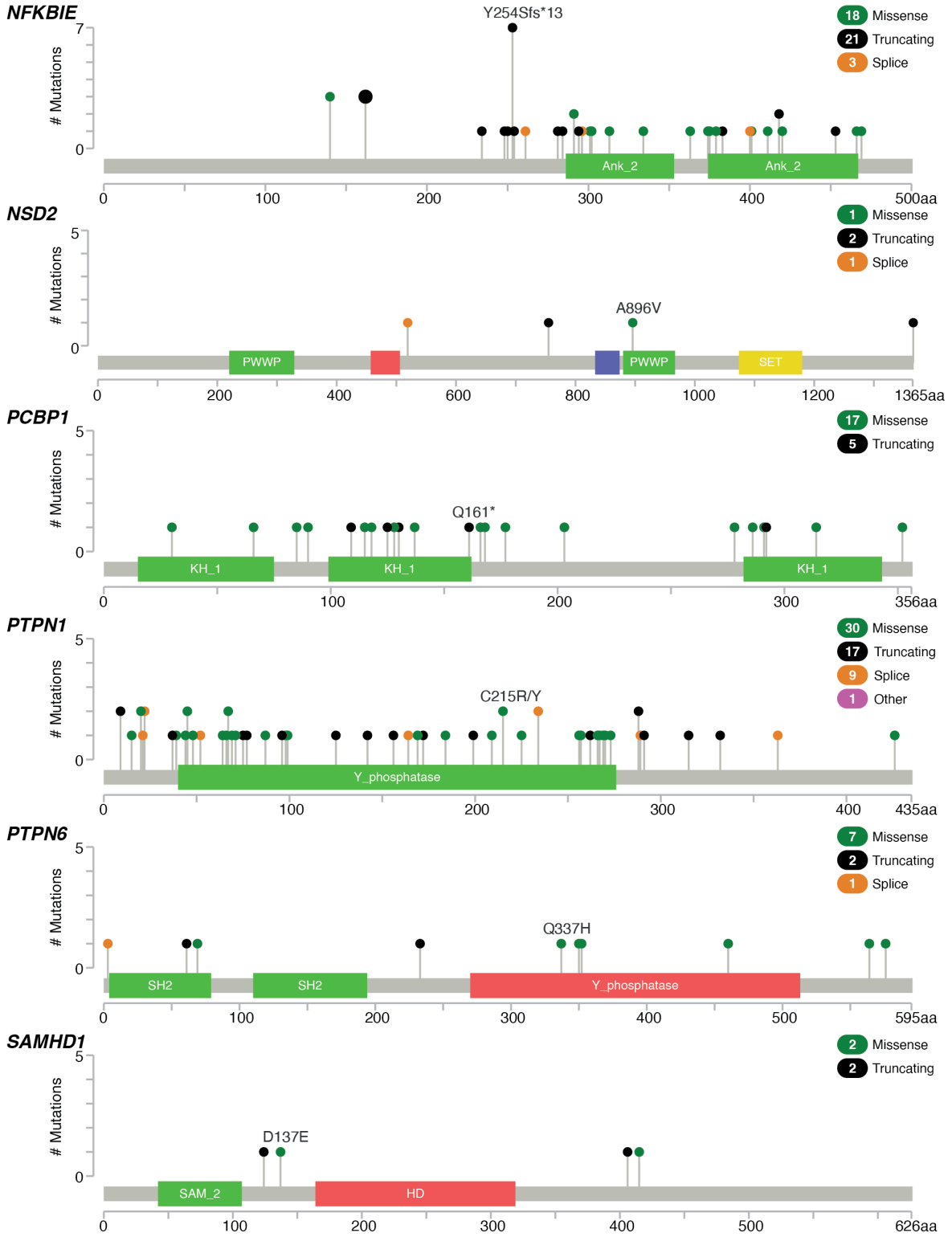
Alig S. *et al.*, ctDNA in cHL



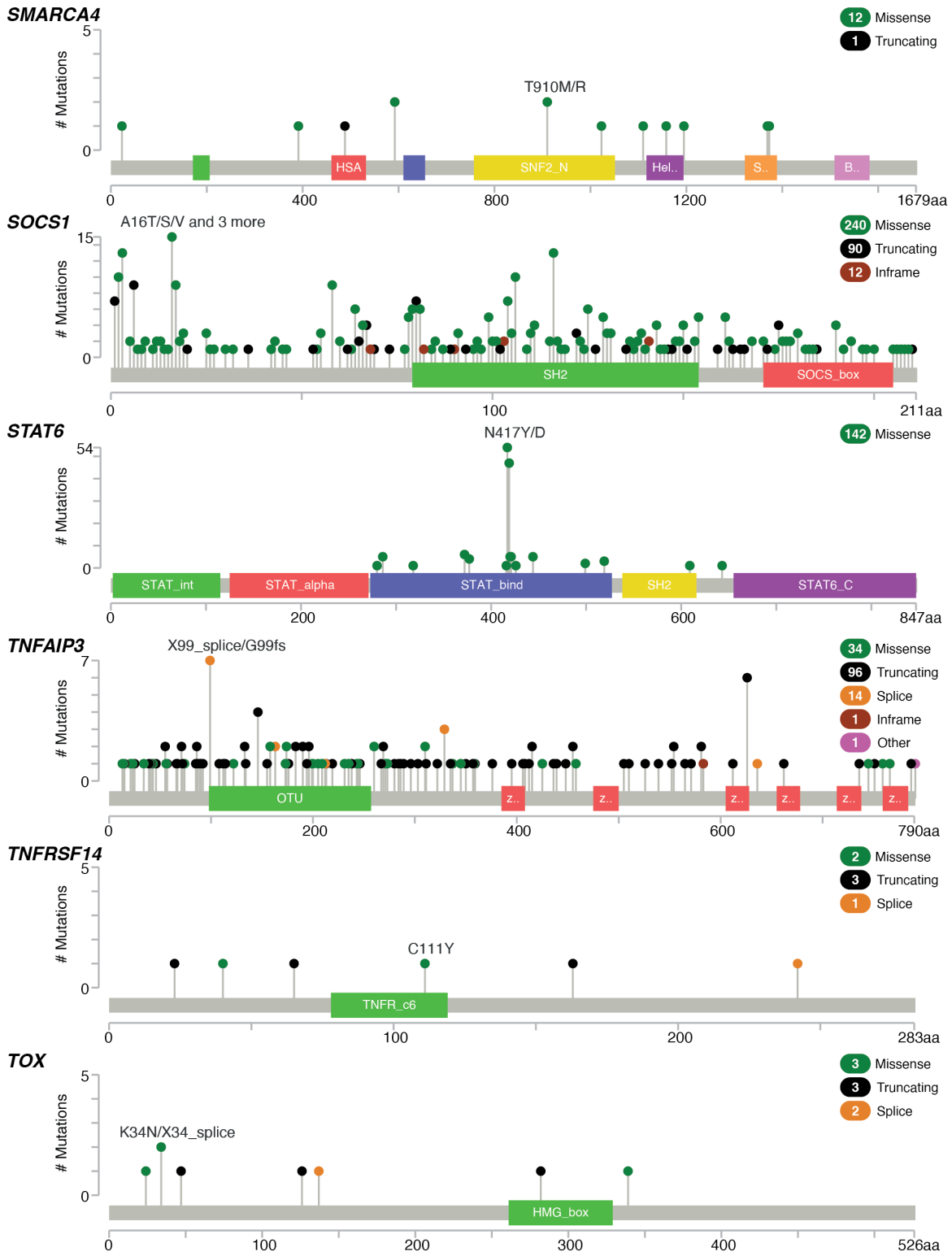
Alig S. *et al.*, ctDNA in cHL

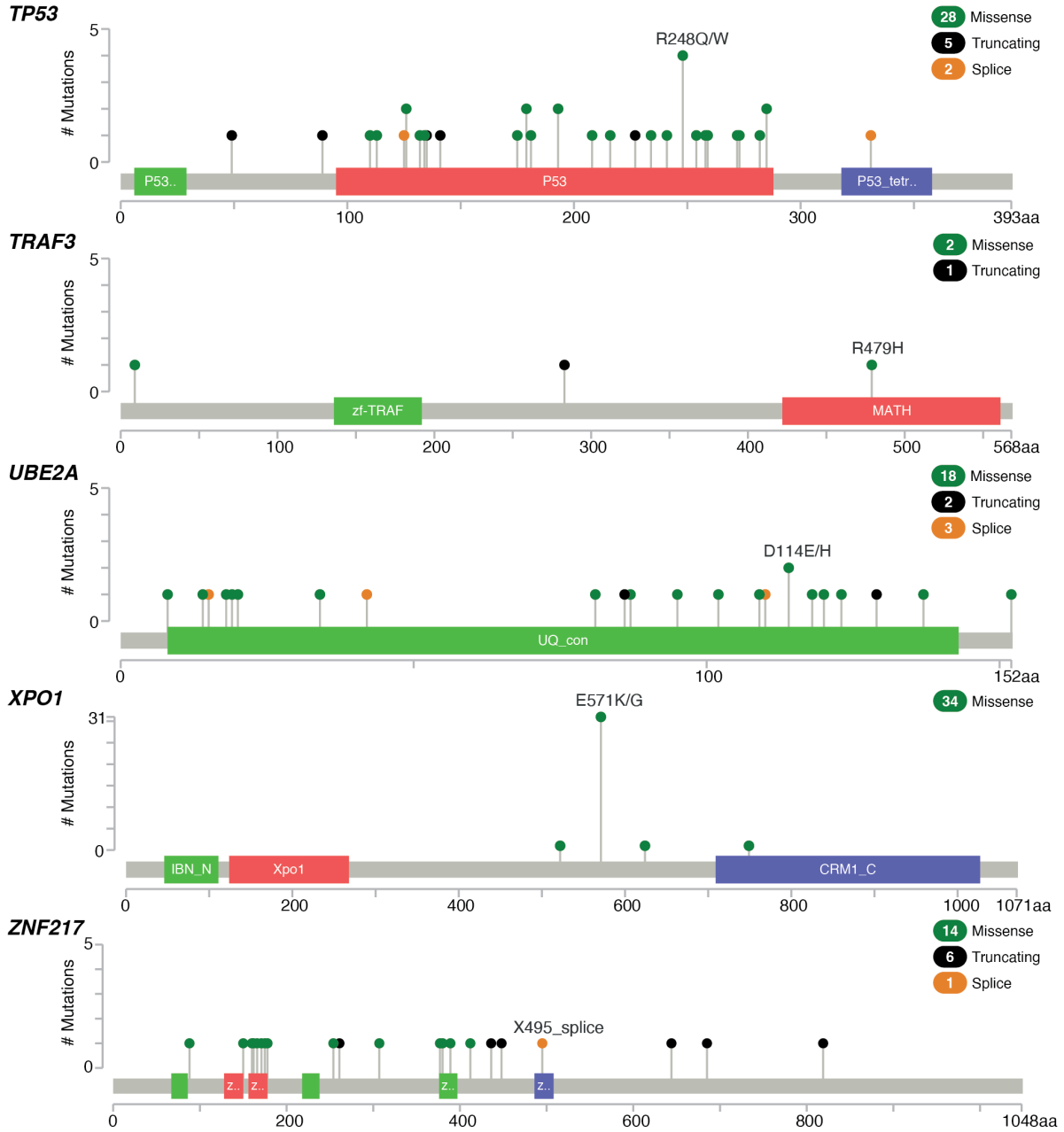


Alig S. *et al.*, ctDNA in cHL



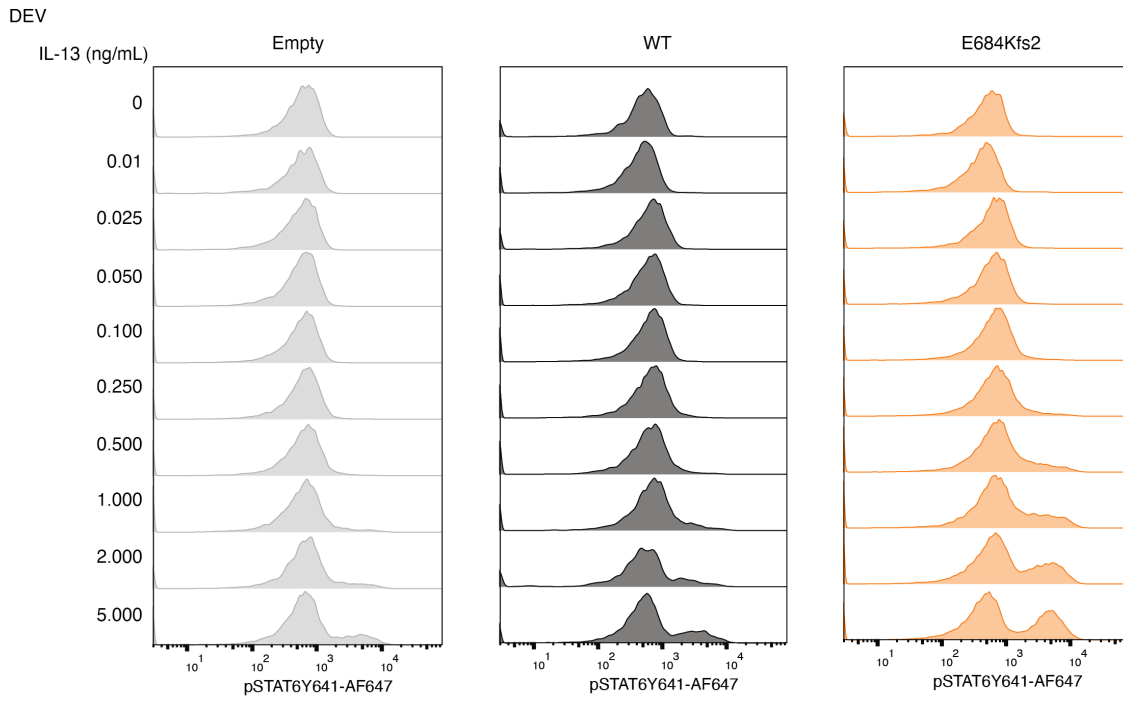
Alig S. *et al.*, ctDNA in cHL



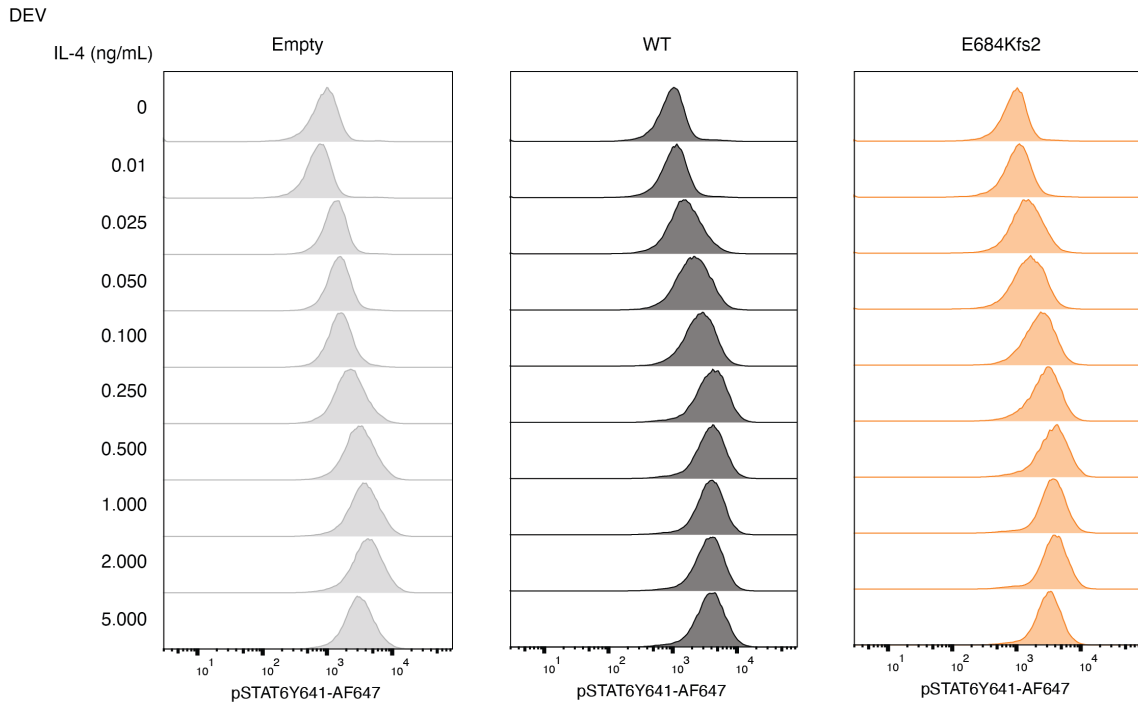


Lollipop plots summarizing non-silent SNVs and Indels in 41 significantly mutated genes identified by MutSig2CV. Mutation types are colour coded as indicated in the graphs. Mutation calls from targeted sequencing are visualized for all but 4 genes which were only covered by whole exome sequencing (*ZNF217*, *CISH*, *NFKB2*, *CD74*).

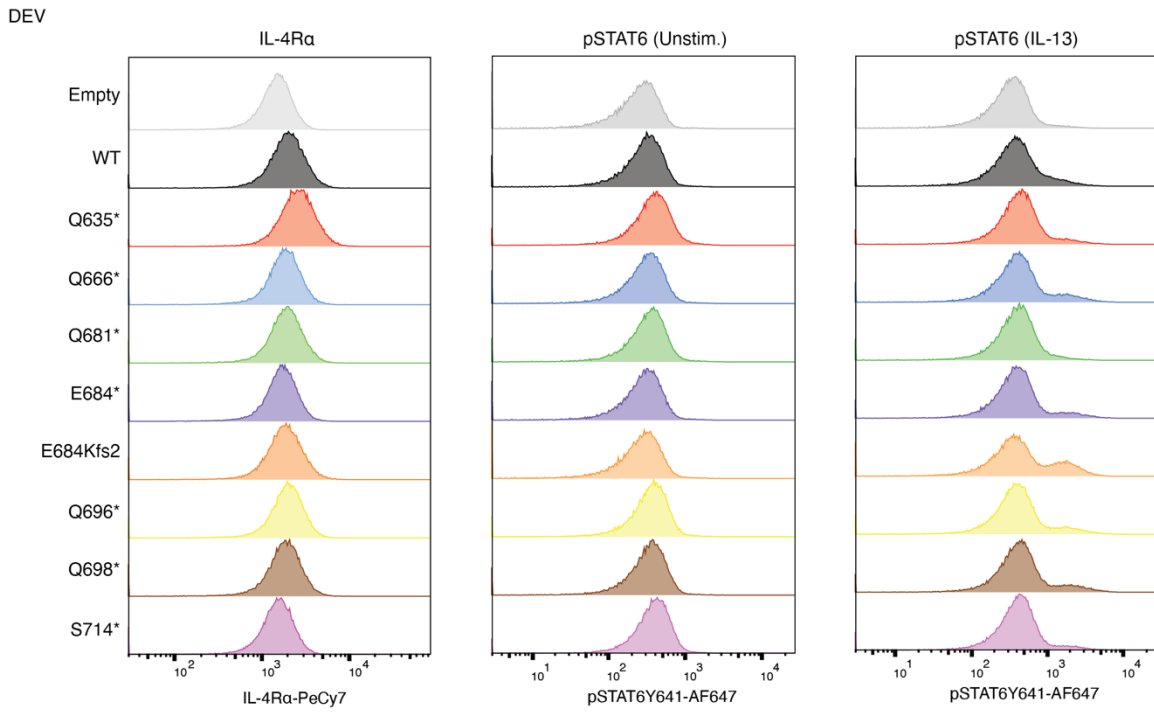
**Supplementary Note Figure 10: Raw cell line flow data.**



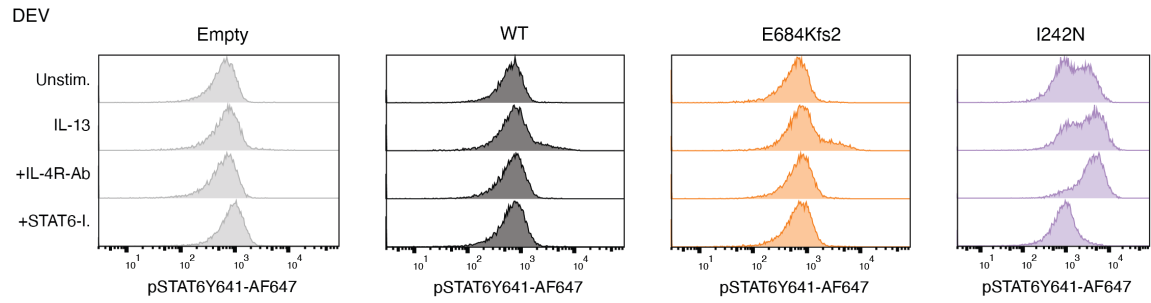
**Supplementary Note Figure 10: Raw cell line flow data (continued).**



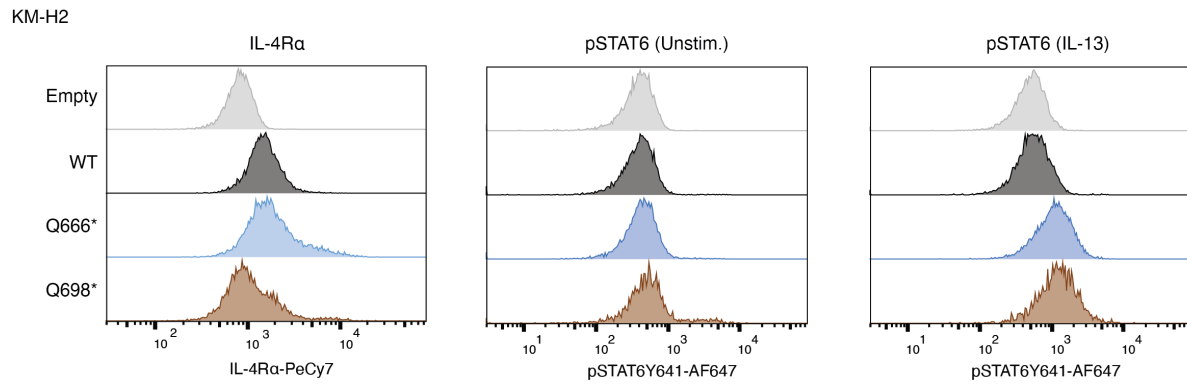
**Supplementary Note Figure 10: Raw cell line flow data (continued).**



**Supplementary Note Figure 10: Raw cell line flow data (continued).**

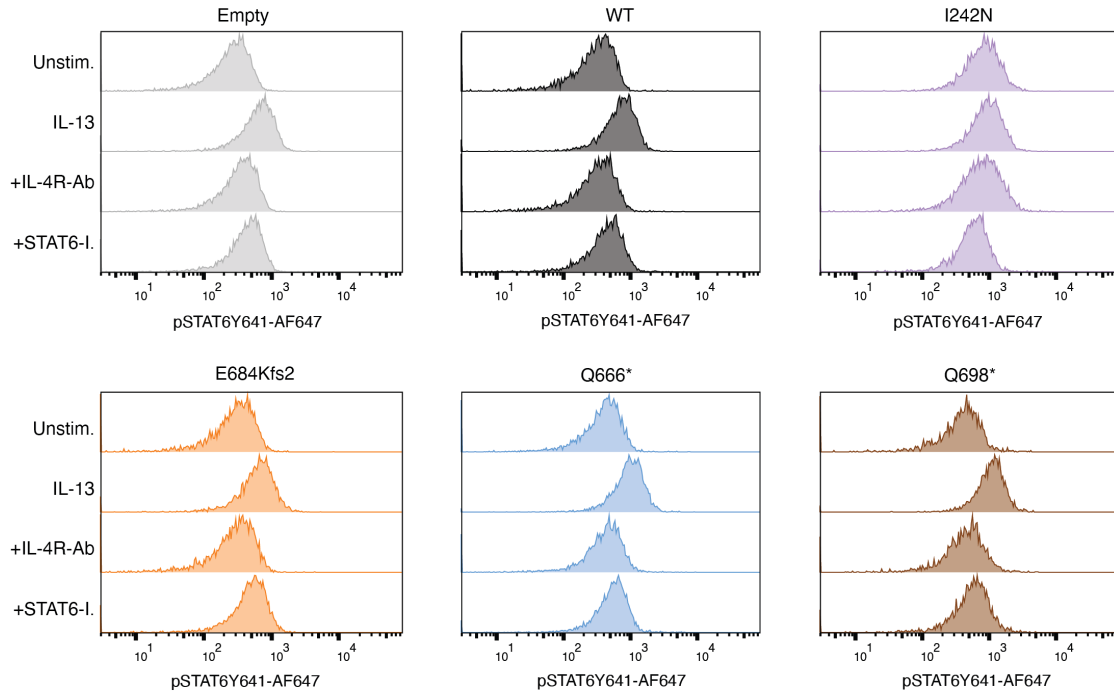


**Supplementary Note Figure 10: Raw cell line flow data (continued).**

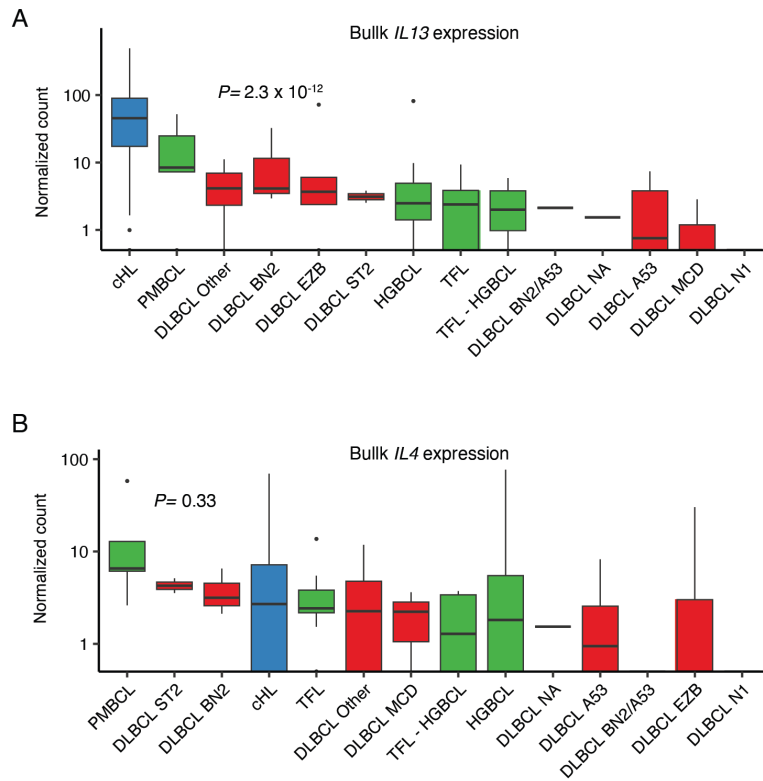


**Supplementary Note Figure 10: Raw cell line flow data (continued).**

KM-H2



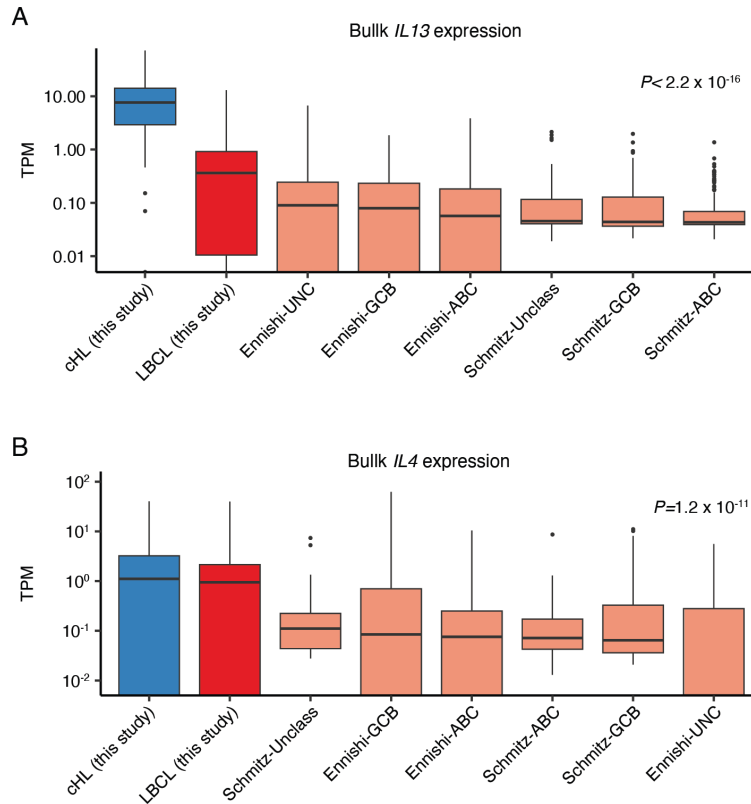
**Supplementary Note Figure 11: Bulk *IL13* and *IL4* expression by histology.**



Boxplot comparing **(A)** *IL13* and **(B)** *IL4* expression by bulk RNA-Sequencing visualized as normalized counts by histology and genetic subtype. Kruskal-Wallis p-value is provided. Subtypes with  $n < 3$  were excluded from statistical testing. Classic Hodgkin Lymphoma (cHL),  $n=86$ ; Diffuse Large B-cell Lymphoma (DLBCL) A53,  $n=8$ ; DLBCL ST2,  $n=2$ ; Transformed Follicular Lymphoma (TFL),  $n=13$ ; DLBCL Other,  $n=12$ ; TFL-High-grade B-cell Lymphoma (HGBCL),  $n=4$ ; DLBCL BN2,  $n=3$ ; HGBCL,  $n=8$ ; DLBCL MCD,  $n=3$ ; Primary Mediastinal B-cell lymphoma (PMBL),  $n=5$ ; DLBCL EZB,  $n=5$ ; DLBCL N1,  $n=1$ ; DLBCL NOS,  $n=1$ ; DLBCL BN2/A53,  $n=1$ .

Each box represents the interquartile range (the range between the 25th and 75th percentile) with the median of the data, whiskers indicate the upper and lower value within 1.5 times the IQR.

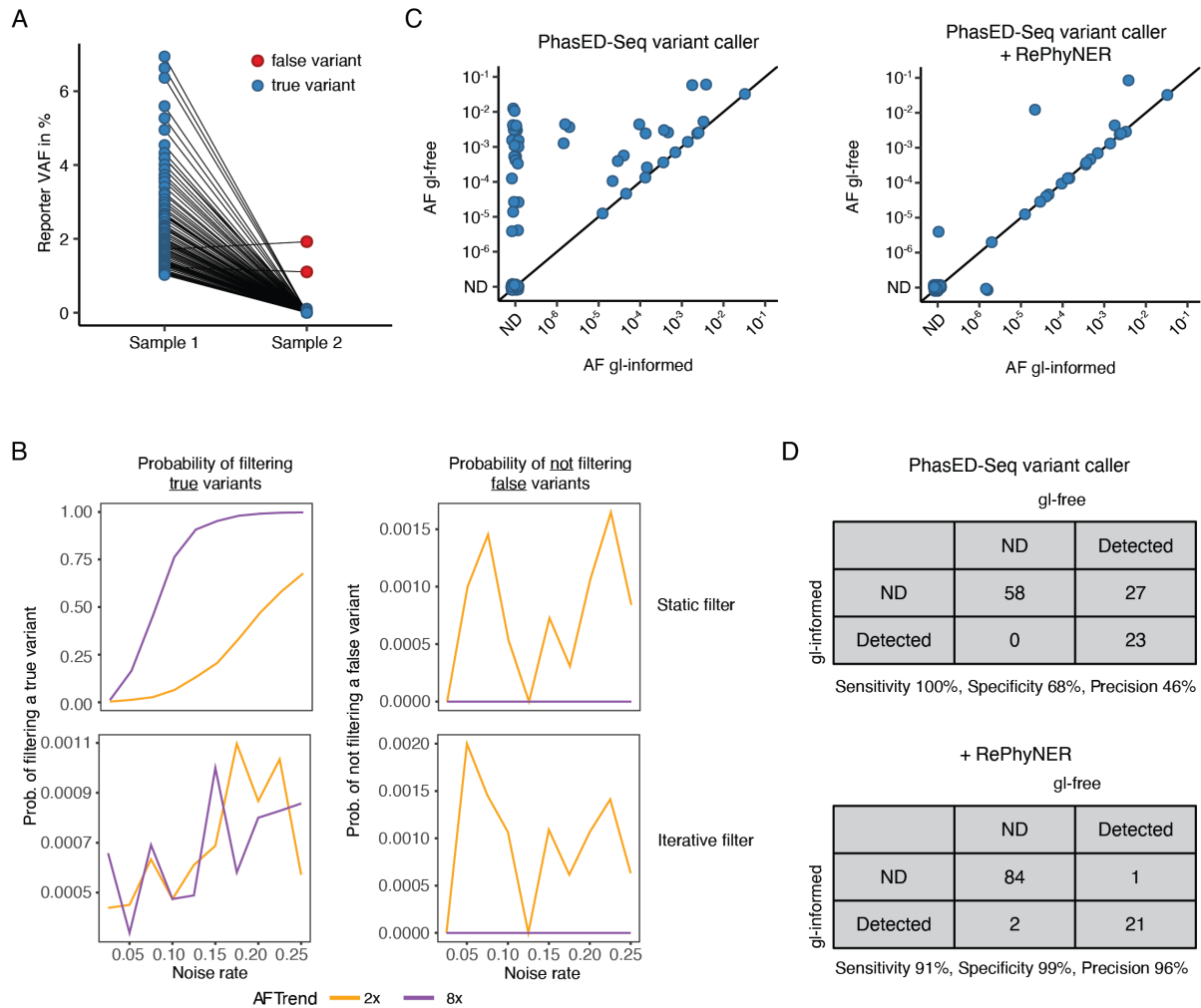
**Supplementary Note Figure 12: *IL13* and *IL4* expression by histology in public datasets.**



(A) *IL13* and (B) *IL4* expression assessed within this study put in context with publicly available datasets. TPM values for overlapping genes reported across datasets were renormalized and visualized. Datasets from Schmitz, *NEJM* 2018<sup>1</sup> and Ennishi, *Journal of Clin Oncol* 2019<sup>2</sup> were used for the analysis. Kruskal-Wallis p-values are provided. cHL (this study): n=86; LBCL (this study): n=66; Ennishi-ABC: n=93; Ennishi-GCB: n=168; Ennishi-UNC: n=33; Schmitz-ABC: n=243; Schmitz-GCB: n=138; Schmitz-UNC: n=100.

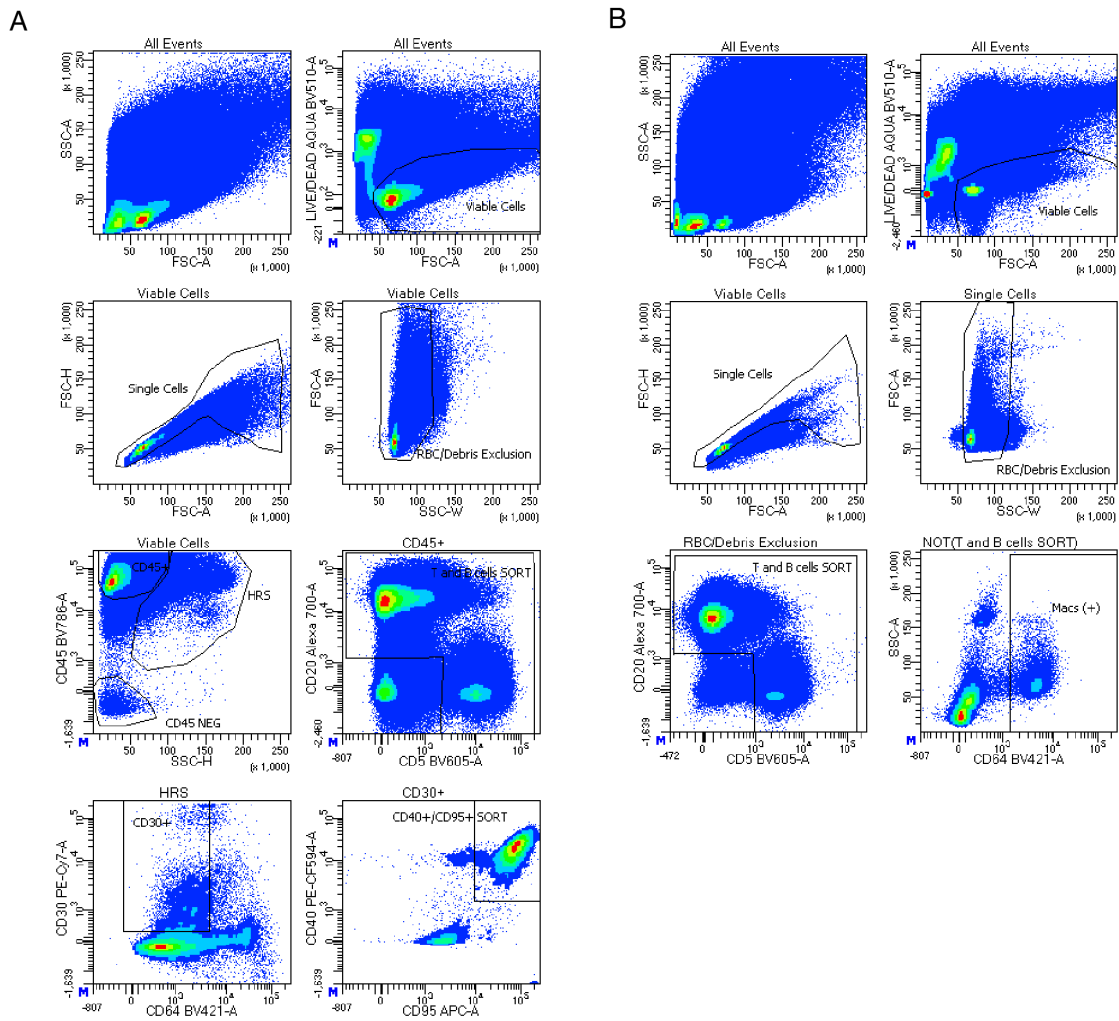
Each box represents the interquartile range (the range between the 25th and 75th percentile) with the median of the data, whiskers indicate the upper and lower value within 1.5 times the IQR.

**Supplementary Note Figure 13: Recursive Phylon Nomination, Enumeration, and Recovery (RePhyNER) to allow for reliable germline-free MRD detection.**



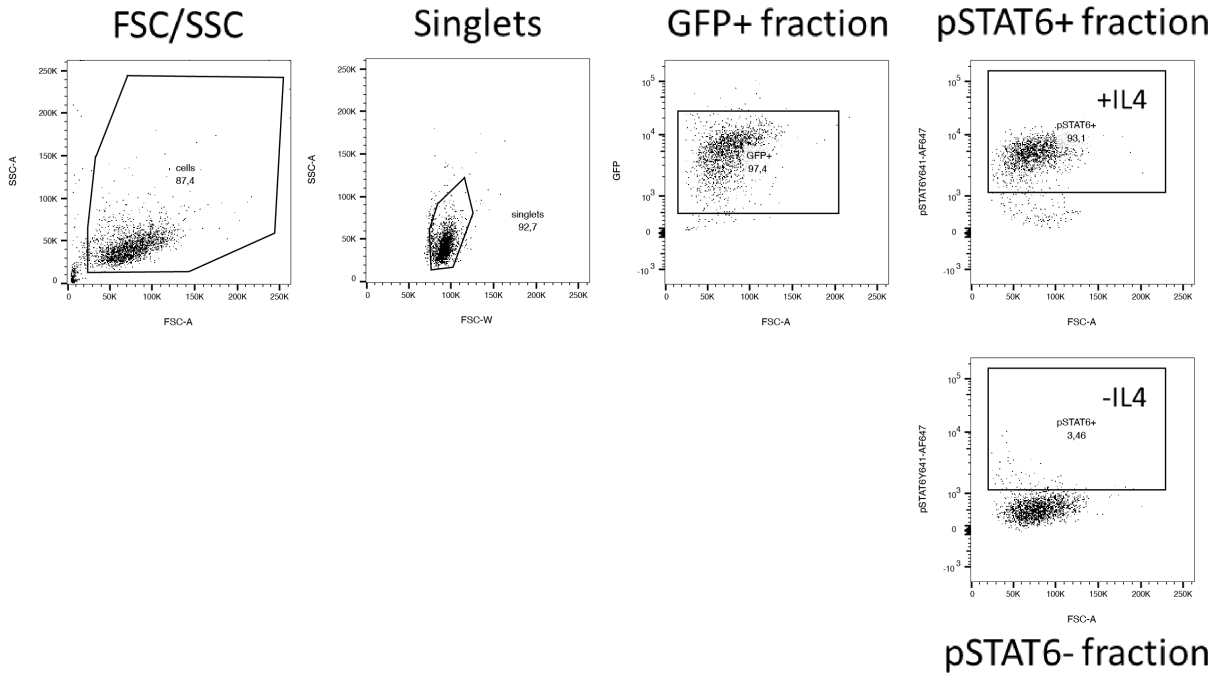
**(A)** Line plots visualizing reporter VAF kinetics between two samples of one exemplar individual. False variants with germline support are coloured in red, while tumour-specific reporters without germline support are coloured in blue. **(B)** Line-plots summarizing simulated probabilities for true (left) and false (right) variant removal as a function of noise rate (x-axis) and sample AF trend (coloured lines) using a static (top) and an iterative (bottom) filter. Noise rate was defined as the fraction of false reporters (e.g. germline or CHIP variants) among all reporters. AF trend denotes the change in mean AF between the pretreatment and on-treatment sample. We here visualize 2- and 8-fold changes in AF. Basic assumptions used for the simulations: 150 reporters/variants, 5,000x unique depth. **(C)** AF estimation in 108 on-treatment samples when using matched germline (gl, x-axis) or when assessed gl-free (y-axis). The left scatter plot shows results generated without iterative filtering, while the right plot visualizes results generated using RePhyNER. ND: Not detected. **(D)** Contingency table summarizing MRD detection as a function of matched germline information (top: without RePhyNER; bottom: with RePhyNER).

Supplementary Note Figure 14: Pre-sorting gates prior to scRNA-Sequencing.



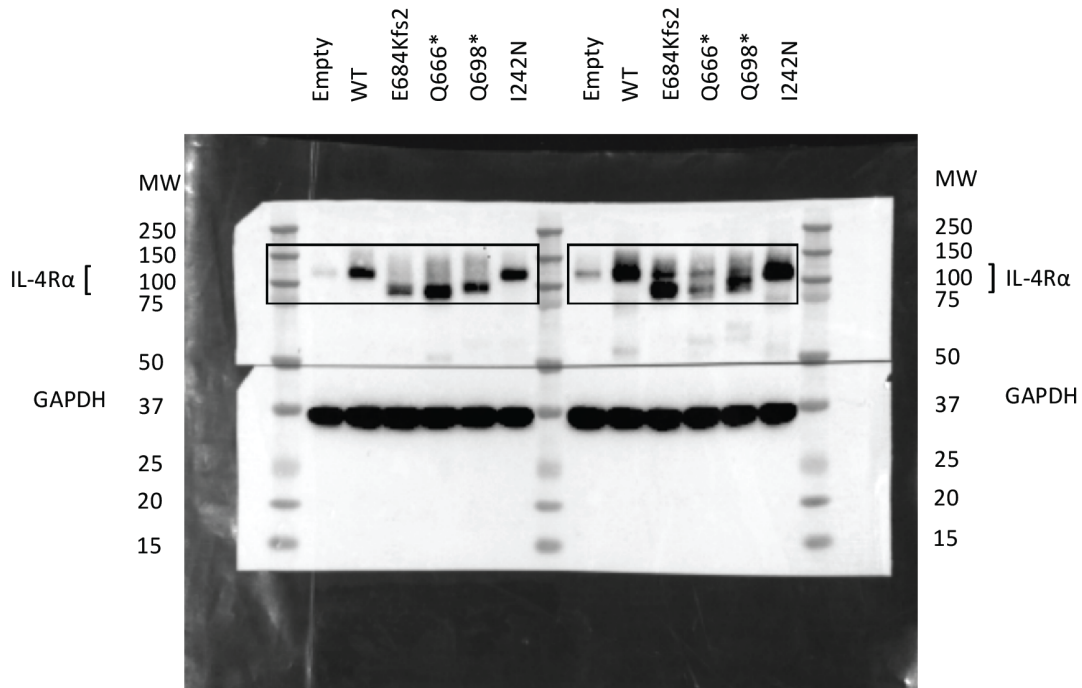
Gating strategy used to pre-sort cells for single-cell RNA-Sequencing as relevant to **Fig. 1H-I** and **Supplementary Note [Fig. 7]**.

**Supplementary Note Figure 15: PhosphoSTAT6 flow gates.**

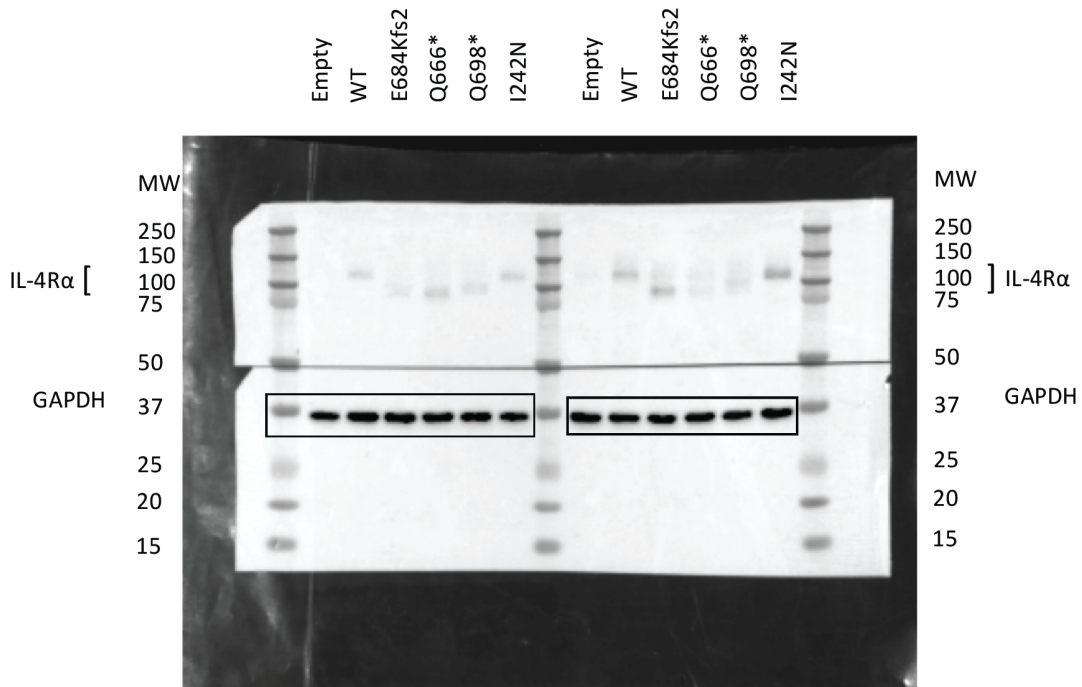


Gating strategy for STATpY641 as applied in **Fig. 4B-E**, **Extended Data Fig. 8D-F** and **Supplementary Note [Fig. 10]**.

**Supplementary Note Figure 16: Full immunoblot scans.**

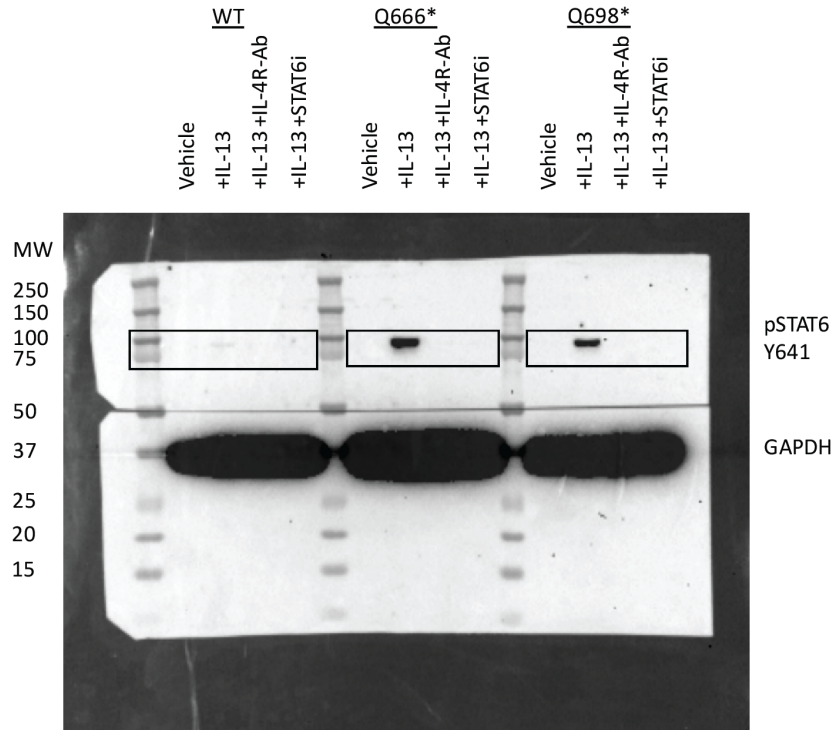


Boxed samples included in manuscript. Other samples are excluded.  
Extended Fig 8A, IL-4Rα

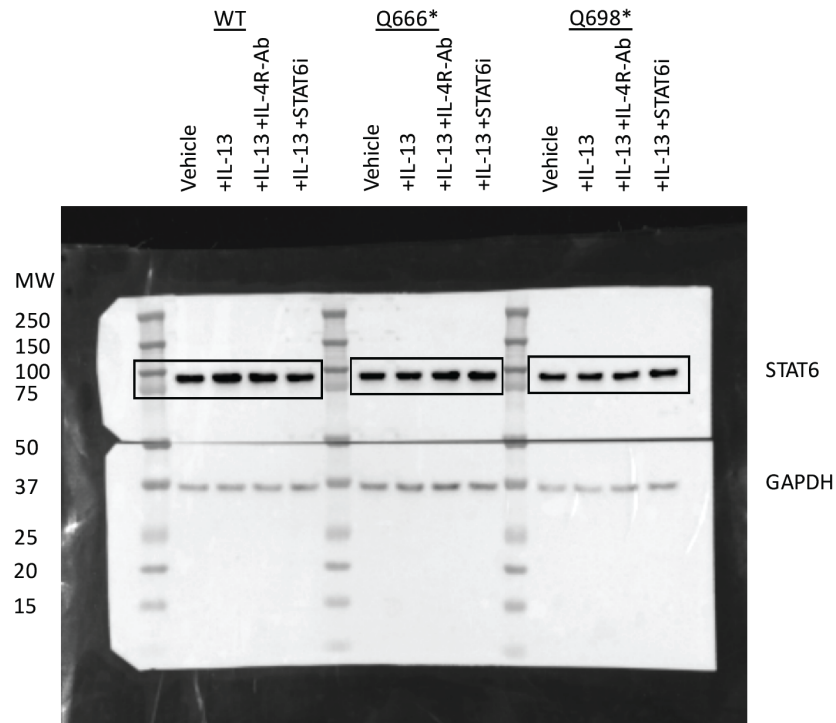


Boxed samples included in manuscript. Other samples are excluded.  
Same blot as 'IL-4Rα', shorter exposure  
Extended Fig 8A, GAPDH

Alig S. *et al.*, ctDNA in cHL

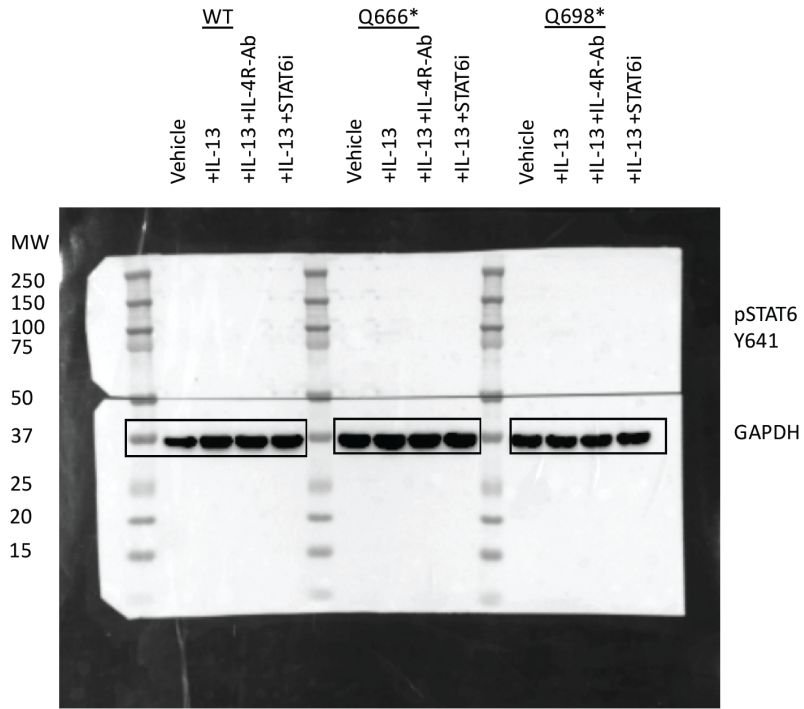


Boxed samples included in manuscript. Other samples are excluded.  
Extended Fig 8G, pSTAT6 Y641



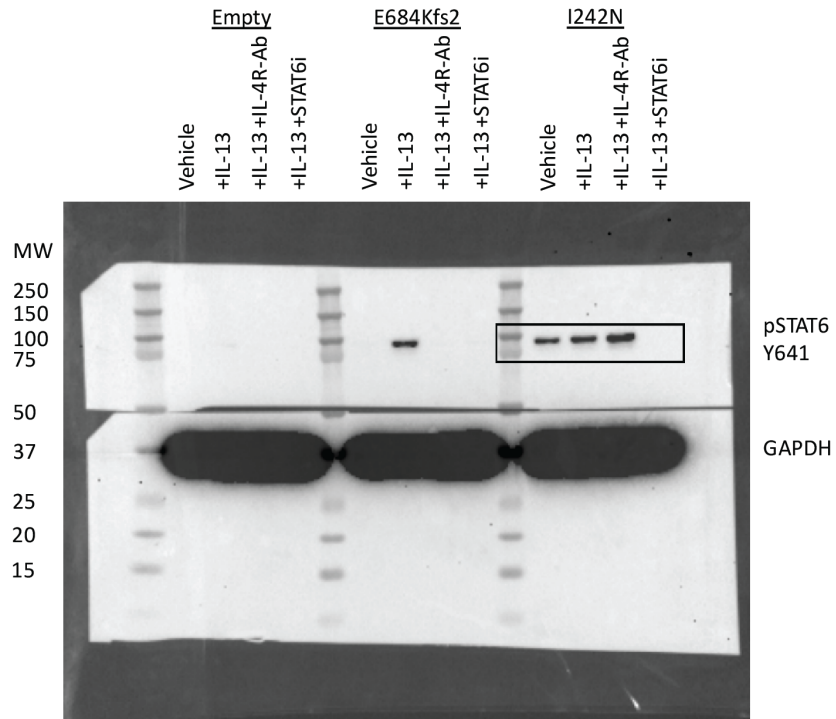
Boxed samples included in manuscript. Other samples are excluded.  
Stripped and reprobed for STAT6 on 'pSTAT6 Y641' blot  
Extended Fig 8G, STAT6

Alig S. *et al.*, ctDNA in cHL

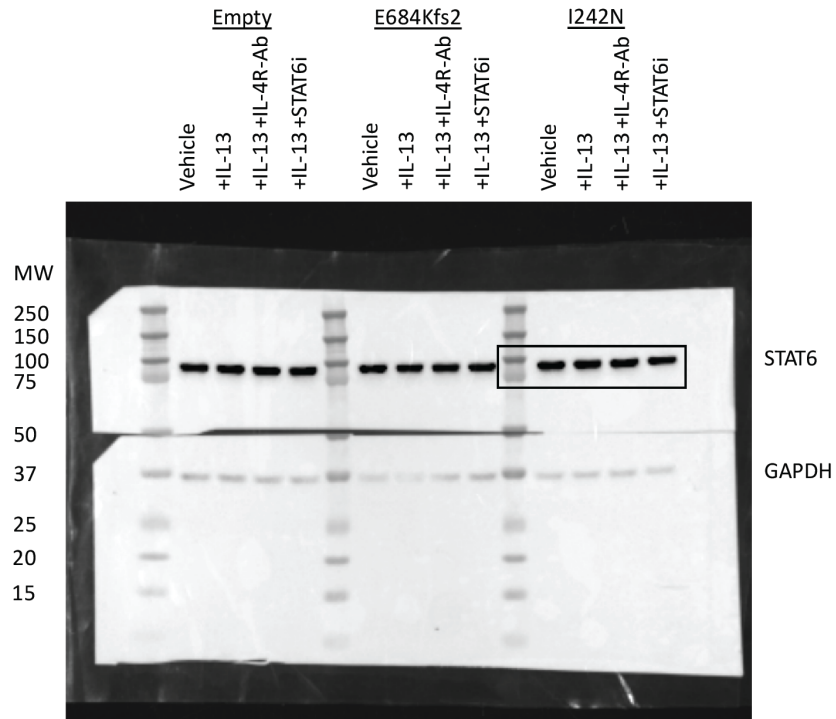


Boxed samples included in manuscript. Other samples are excluded.  
Same blot as 'pSTAT6 Y641', shorter exposure  
Extended Fig 8G, GAPDH

Alig S. *et al.*, ctDNA in cHL

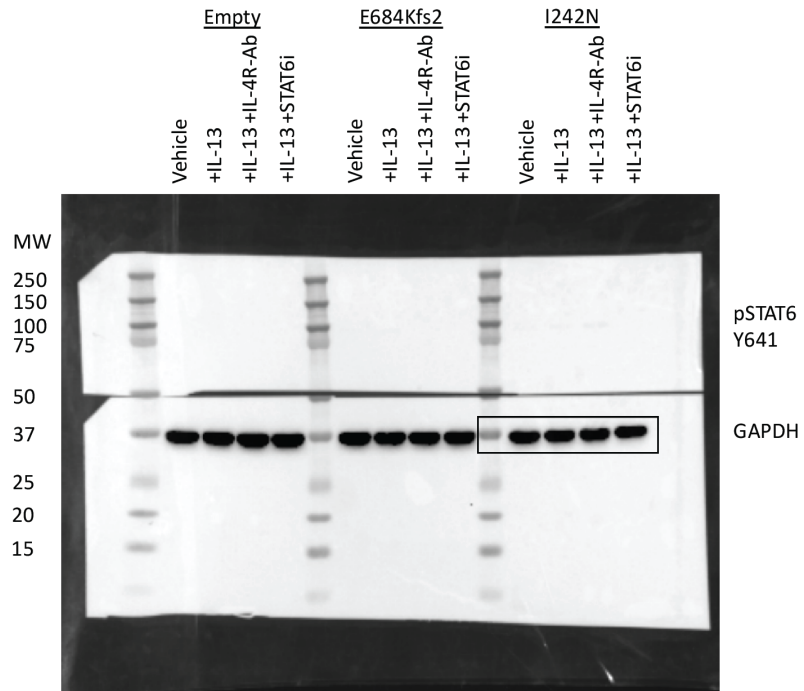


Boxed samples included in manuscript. Other samples are excluded.  
Extended Fig 8H, pSTAT6 Y641



Boxed samples included in manuscript. Other samples are excluded.  
Stripped and reprobed for STAT6 on 'pSTAT6 Y641' blot  
Extended Fig 8H, STAT6

Alig S. *et al.*, ctDNA in cHL



Boxed samples included in manuscript. Other samples are excluded.  
Same blot as 'pSTAT6 Y641', shorter exposure  
Extended Fig 8H, GAPDH

## REFERENCES

- 1 Schmitz, R. *et al.* Genetics and Pathogenesis of Diffuse Large B-Cell Lymphoma. *N Engl J Med* **378**, 1396-1407 (2018). <https://doi.org:10.1056/NEJMoa1801445>
- 2 Ennishi, D. *et al.* Double-Hit Gene Expression Signature Defines a Distinct Subgroup of Germinal Center B-Cell-Like Diffuse Large B-Cell Lymphoma. *Journal of Clinical Oncology* **37**, 190-201 (2019). <https://doi.org:10.1200/jco.18.01583>